NASA TECHNICAL NOTE

NASA TN D-7769

NASA TN D-7769

ANALYTICAL CHEMICAL KINETIC INVESTIGATION OF THE EFFECTS OF OXYGEN, HYDROGEN, AND HYDROXYL RADICALS ON HYDROGEN-AIR COMBUSTION

by George T. Carson, Jr.

Langley Research Center
Hampton, Va. 23665

NATIONAL AERONAUTICS AND SPACE ADMINISTRATION • WASHINGTON, D. C. • NOVEMBER 1974

1. Report No.	2. Government Accession No.	3. Recipient's Catalog No.
NASA TN D-7769		

4. Title and Subtitle	5. Report Date
ANALYTICAL CHEMICAL KINETIC INVESTIGATION OF THE EFFECTS OF OXYGEN, HYDROGEN, AND HYDROXYL RADICALS ON HYDROGEN-AIR COMBUSTION	November 1974
	6. Performing Organization Code

7. Author(s)	8. Performing Organization Report No.
George T. Carson, Jr.	L-9576
	10. Work Unit No.
9. Performing Organization Name and Address	505-05-42-01
NASA Langley Research Center Hampton, Va. 23665	11. Contract or Grant No.
	13. Type of Report and Period Covered
12. Sponsoring Agency Name and Address	Technical Note
National Aeronautics and Space Administration Washington, D.C. 20546	14. Sponsoring Agency Code

15. Supplementary Notes

16. Abstract

Quantitative values have been computed which show the effects of the presence of small amounts of oxygen, hydrogen, and hydroxyl radicals on the finite-rate chemical kinetics of premixed hydrogen-air mixtures undergoing isobaric autoignition and combustion. The free radicals were considered to be initially present in hydrogen-air mixtures at equivalence ratios of 0.2, 0.6, 1.0, and 1.2. Initial mixture temperatures used in this investigation were 1100 K, 1200 K, and 1500 K, and pressures were 0.5, 1.0, 2.0, and 4.0 atm. Of the radicals investigated, atomic oxygen was found to be the most effective for reducing induction time, defined as the time to 5 percent of the total combustion temperature rise. The reaction time, the time between 5 percent and 95 percent of the temperature rise, is not decreased by the presence of free radicals in the initial hydrogen-air mixture. Fuel additives which yield free radicals might be used to effect a compact supersonic combustor design for efficient operation in an otherwise reaction-limited combustion regime.

17. Key Words (Suggested by Author(s))	18. Distribution Statement
Chemical kinetics Effects of O, H, and OH Hydrogen-air combustion	Unclassified – Unlimited STAR Category 33

19. Security Classif. (of this report)	20. Security Classif. (of this page)	21. No. of Pages	22. Price*
Unclassified	Unclassified	63	$3.75

*For sale by the National Technical Information Service, Springfield, Virginia 22151

ANALYTICAL CHEMICAL KINETIC INVESTIGATION OF THE EFFECTS OF OXYGEN, HYDROGEN, AND HYDROXYL RADICALS ON HYDROGEN-AIR COMBUSTION

By George T. Carson, Jr.
Langley Research Center

SUMMARY

Quantitative values have been computed which show the effects of oxygen, hydrogen, and hydroxyl radicals on the finite-rate chemical kinetics of premixed hydrogen and air undergoing isobaric combustion. Mole fractions equal to 10^{-6}, 10^{-5}, and 10^{-4} of the free radicals were considered to be initially present, either singly or in combination, in homogeneous, hydrogen-air mixtures with equivalence ratios of 0.2, 0.6, 1.0, and 1.2. Initial temperatures were 1100 K, 1200 K, and 1500 K and pressures were 0.5, 1.0, 2.0, and 4.0 atm. A few other initial states were used when necessary to determine intermediate trends. The investigation demonstrates that small amounts of radicals reduce induction time, herein defined as the time to 5 percent of the temperature rise from the initial mixture temperature to the calculated equilibrium temperature. Also, the study shows that within the range of conditions investigated, hydroperoxyl (HO_2) plays a significant role in the early part of the ignition process; the inflection in its rate of formation can be used to define induction time. The reaction time, defined as time between 5 percent and 95 percent of the temperature rise, is not affected by the initial amounts of free radicals. All of the radicals are more effective in reducing induction time at low initial temperatures. For all mixtures and states, atomic oxygen is the most effective radical of the radicals investigated. The results represent equilibrium chemistry, finite-rate chemical kinetics, and curve-fitting computer programs over this range of conditions. It is also implied that additives which yield free radicals can be used to effect a compact combustor design or to permit operation in otherwise reaction-limited regimes of initial pressures and temperatures.

INTRODUCTION

In support of the NASA Hypersonic Research Engine Project, discussed in reference 1, an analytical chemical kinetic investigation of the effects of free radicals on hydrogen-air combustion was conducted. The most difficult problem areas in the design of the hypersonic ramjet engines are associated with the combustion process. The flow

through the combustor is continuous and supersonic and is composed of mixing and of burning fuel and air. The fuel injection and mixing parts of the processes are extremely important, and in diffusion controlled combustion they control heat release. Where the mixture of fuel and air at the beginning of the combustor is near the threshold temperature for autoignition, the combustion kinetics plays a major part in ignition. In order to minimize the combustor length (thus lowering weight and overall heat transfer), shortening the time for completion of the combustion reaction is critically important.

The initial testing of supersonic combustion ramjet engines will be in ground-based facilities. The high-temperature air required for simulation can be obtained by first heating nitrogen and then mixing it with oxygen. Another method of producing a hot test gas is to burn fuel in a high-pressure oxygen-rich airstream. The combustion process in the burner, or "heater," produces a hot-gas flow whose composition has the proper percentage of oxygen to simulate air. The main difficulty with the latter method is that the air ingested by the test engine contains combustion products, as well as unrecombined free radicals; this may produce misleading test results.

The time for combustion (i.e., the total time associated with completion of the chemistry of combustion) is usually divided into two parts: induction time and reaction time. For induction time, investigators sometimes use a criterion based on reaching a prescribed concentration level of some product species (ref. 2 uses the hydroxyl radical at the level of 10^{-6} mole per liter), or one based on the rate of temperature rise due to three-body radical recombination (ref. 3), or one based on experimentally measured light emission or absorption (ref. 4). In the present paper, as in reference 5, induction time is defined as the time to reach 5 percent of the equilibrium temperature rise, i.e., 5 percent of the difference between the initial static temperature of the mixture and the equilibrium temperature. The reaction time is the remainder of the time required to achieve complete combustion. However, since the chemical process approaches completion asymptotically, the latter part of the heat release is lost in the exhaust of a scramjet. Therefore, for the purpose of this paper, a finite limit for the reaction was chosen to be 95 percent of the potential temperature rise. Reference 5 includes a limited comparison of the induction times of hydrogen-air mixtures with and without initial amounts of the free radicals, oxygen (O), hydrogen (H), and hydroxyl (OH). It is shown that the presence of initially small amounts of free radicals results in a significant reduction of induction time. The present analysis was undertaken in an attempt to improve the understanding of the significance of small amounts of contaminants in combustible gaseous mixtures.

Only the chemical kinetics of a premixed one-dimensional stream of hydrogen and air is considered here. Elimination of injection and mixing was considered a necessary

simplification in order to achieve the objectives. The chemical kinetic analyses of hydrogen-air combustion at constant pressure (diverging combustor) which are presented show the effects of small amounts of atomic oxygen, atomic hydrogen, or hydroxyl radical on the induction and reaction times. The range of thermodynamic state points and compositions included are typical of ramjet operation. The scope of the computer programs used in this analysis precluded the investigation of mixing length and local equivalence ratio variance.

SYMBOLS

I	number of chemical species
i	specific chemical species
j	finite-rate reaction
k_j	reaction rate constant for reaction j
k_{-j}	reaction rate constant for reverse of reaction j
M_i	molecular mass of species i
p	static pressure (1 atm = 101 325 Pa)
R	universal gas constant, 8.31434 J/mol-K
T	static temperature, K
T_f	equilibrium temperature, K
T_m	mean static temperature, $\frac{1}{2}(T_1 + T_f)$, K
T_1	initial static temperature, K
t	time, μsec
X_e	effective mole fraction of radical species

X_i	mole fraction of specific chemical species, $\frac{\text{Moles of species i}}{\text{Moles of mixture}}$
Y_i	mass fraction of specific chemical species, $\frac{\text{Mass of species i}}{\text{Mass of mixture}}$
$\Delta\tau$	induction-time difference, $\tau_o - \tau$, μsec
$\Delta\tau/\tau_o$	relative reduction in induction time
θ	fractional temperature rise, $(T - T_1)/(T_f - T_1)$
τ	induction time of a mixture (time at which $\theta = 0.05$), μsec
τ_o	induction time of a mixture not containing initial quantities of free radicals O, H, or OH, μsec
τ_r	reaction time (time to $\theta = 0.95$ less time to $\theta = 0.05$), μsec
$\tau_r p^{1.641}$	reaction-time parameter, μsec-(atm)$^{1.641}$
ϕ	equivalence ratio, $\frac{\text{Fuel-air ratio}}{\text{Stoichiometric fuel-air ratio}}$

ANALYSIS

In order to obtain numerical values used in this analysis, two different computer programs were used. First, the equilibrium chemistry program (ref. 5) determines the equilibrium temperature and composition for mixtures at given initial temperatures and composition under isobaric conditions. Second, the chemical kinetics program (also by the authors of ref. 5) determines temperature and composition in mixtures reacting at finite rates. An isobaric, premixed, one-dimensional adiabatic flow is assumed.

Four classes of gaseous mixtures were considered:

(1) Air: As a basic simplifying assumption, assume air to consist only of nitrogen and oxygen; this seems justified since other gases are present only in small amounts and the radicals to be investigated are not present. Reference 6 indicates that air contains 20.9472-percent oxygen and 79.0528-percent nitrogen by volume. Also, since the molec-

ular weight of air is given as a constant to an altitude of 90 km in reference 6, the composition of air is assumed to be constant.

(2) Stoichiometric fuel-air mixture: A stoichiometric mixture of fuel and air is one in which both reactants can react completely to form products. The stoichiometric hydrogen-oxygen reaction is indicated by the equation

$$2H_2 + O_2 = 2H_2O$$

The oxygen-hydrogen ratio in a stoichiometric mixture is determined by the relationship

$$Y_i = \frac{X_i M_i}{\sum_{i=1}^{I} X_i M_i}$$

which gives

$$\frac{Y_{O_2}}{Y_{H_2}} = 7.936507$$

The nitrogen-oxygen mass-fraction ratio for air is similarly determined as

$$\frac{Y_{N_2}}{Y_{O_2}} = 3.3103448$$

From the definition of mass fraction it is known that

$$\sum_{i=1}^{I} Y_i = Y_{N_2} + Y_{O_2} + Y_{H_2} = 1$$

The three unknown quantities can be found from the preceding three equations. The formation of oxides of nitrogen below 3000 K for short residence times is assumed negligible.

(3) Nonstoichiometric fuel-air mixtures: The mass fractions of nitrogen, oxygen, and hydrogen for nonstoichiometric compositions are computed in a similar manner. The difference is the inclusion of an equivalence ratio ϕ which in this report is defined as

$$\phi = \frac{\left(Y_{H_2}/Y_{O_2}\right)}{\left(Y_{H_2}/Y_{O_2}\right)_{\text{stoichiometric}}}$$

An equivalence ratio of unity signifies stoichiometric proportions, less than unity implies a fuel-lean mixture, and greater than unity implies a fuel-rich mixture. The composition of baseline mixtures in mass fractions is shown in table 1.

(4) Small amounts of initial free radicals: Finally, both stoichiometric and non-stoichiometric mixtures were calculated that had small (typically, 10^{-6} to 10^{-4}) mole fractions of free radicals, O, H, and OH, initially present.

The chemical reactions and rate constants k_j in this analysis are shown in table 2, along with their sources (refs. 7 to 16). Although rate constants and third-body efficiencies used in the chemical kinetics program may be easily changed, the reactions themselves cannot be changed without reprograming. For the investigation this was not considered to be a drawback because the relative effect of free radicals was of prime importance. Since the effects of the free-radical reactions with hydrogen peroxide and hydroperoxyl are small above 1100 K, they were not included in the analysis. At the time of the preparation of the present paper, the authors of reference 16 experimentally determined a new value of k_{12}; this new value is designated herein as k_{12A}. The third-body efficiencies are given in reference 5. The value for reaction 8 is set at unity in order to establish a baseline reacting mixture which does not depend upon water as a third body.

The first parameter derived from the computational values was a fractional temperature rise which was defined as

$$\theta = \frac{T - T_1}{T_f - T_1}$$

This parameter expresses quantitatively the amount of reaction corresponding to a change in the mixture temperature. In this investigation, as in reference 5, induction time τ is defined as the time at which $\theta = 0.05$ and the total reaction time is defined by $\theta = 0.95$. Another parameter used is the relative reduction of induction time. It has been given the symbol $\Delta\tau/\tau_0$ and is defined as the ratio of the difference between the induction time of a mixture with and without initial free radicals $\Delta\tau = \tau - \tau_0$ to the induction time without initial free radicals.

The computed values of the relative reduction of induction time and their relationships with the prime parameters of this study are discussed in the following section.

RESULTS AND DISCUSSION

Equilibrium Chemistry Computations

The results of the computations, as shown in figures 1 to 4, give equilibrium temperature as a function of initial temperature along isobars for each of the equivalence

ratios. These curves are valid with or without initial amounts of free radicals up to 10^{-4} mole per mole of mixture.

Finite-Rate Chemistry Computations

Temperature-time mapping.- Figures 5 to 8 map static temperature as a function of time for a constant-pressure combustion process. Shown are lines of constant initial temperature and fractional temperature rise. These figures demonstrate the importance of initial temperature. Below 1000 K the induction time becomes so great that the fuel-air mixture cannot ignite during the residence time of about 250 μsec. Figures 5, 6, 7, and 8 represent examples at which the static pressures p are 0.5, 1.0, 2.0, and 4.0 atm, respectively; and comparison of the data of these figures shows that increasing pressure decreases induction time. This seems to be generally true except for low initial static temperature (i.e., near 1100 K) where increasing pressure has an inhibiting effect, as is clearly depicted by figures 7 and 8. For $T_1 = 1100$ K, $p = 4.0$ atm, $\phi = 1.0$, and $\theta = 0.5$, ignition did not occur even beyond 1000 μsec.

Table 3 is a presentation of input values (ϕ, T, p, X_O, X_{H_2}, and X_{OH}) and the resulting induction times and related fractions (τ, τ/τ_0, and $\Delta\tau/\tau_0$). Since atomic oxygen produced the most dramatic results, it was used for graphic presentation.

Figure 9 shows the effect a 10^{-4} mole fraction of atomic oxygen has on combustion. In comparing this figure with figure 6, it is noted that the presence of initial radicals has an acceleration effect on combustion which is large for low initial temperature but is negligible for high initial temperature. Because of the large range in magnitude of the parameter, graphs subsequent to figure 9 are plotted on logarithmic scales.

Induction-time mapping.- Figures 10, 11, and 12 show the variation of induction time with static pressure for families of initial temperature, equivalence ratio, and initial trace amount of radical, respectively. From figure 10 it is apparent that the effect of initial temperature is large. For initial temperatures of 1200 K (and below) there are definite minimum induction times. For 1500 K and above, no minimum occurs below 10 atm. According to reference 15 this is because reaction 9 inhibits the hydrogen-air reaction at low temperature and high pressure. The effect of equivalence ratio is minor, as may be observed from figure 11. The pronounced effect of small amounts (10^{-6}, 10^{-5}, and 10^{-4}) of initial atomic oxygen is shown in figure 12.

Time variation of species.- The variation of species mass fraction with time is shown in figures 13 to 18. Figure 13 depicts a stoichiometric mixture of hydrogen and air initially at 1100 K and without any initial radicals. The increase of products (radicals and H_2O) is very rapid. Figure 14 shows the results of adding small amounts of radicals and indicates that the formation of products begins much sooner when the radicals are present. However, the rate of change of species mass fraction with time is

much less. The chemical-kinetics program shows that the reactions containing atomic oxygen begin at a low temperature and, being initially of small magnitude, produce little temperature rise to increase the reaction rates. Comparison of figures 13, 15, and 17 shows that, for increasing initial temperature (i.e., 1100, 1200, and 1500 K, respectively), the products form sooner even though the rate of change is less; also, when the comparison is expanded to include figures 14, 16, and 18, the product-forming action of atomic oxygen becomes less pronounced as the initial temperature is increased. In figures 14(a), 16(a), and 18(a), which cover the first part of the reaction only, it is observed that the amount of atomic oxygen actually decreases at first. This pheonmenon is apparently because of reaction 7 which results in removal of atomic oxygen and hydrogen. Figures 13(a), 15(a), and 17(a) show that all products monotonically increase for mixtures which do not contain initial atomic oxygen.

Hydroperoxyl relation to induction time.- It was observed that the peak of hydroperoxyl formation occurred near the selected induction time criterion of $\theta = 0.05$. This trend was investigated for cases which have large induction times, i.e., low initial temperature and high pressure. Figures 19 and 20 show that this trend holds. Therefore, it appears that the peak of hydroperoxyl formation is a good indicator for finding the induction time. For the range of temperature and pressure investigated, the two equations shown in table 2 involving hydroperoxyl appear to be sufficient.

Figure 21 shows the relationship between induction time and static pressure as calculated with and without the formation of hydroperoxyl. It is evident from the figure that computations which do not include hydroperoxyl give increasingly erroneous results as the static pressure increases. According to reference 17, HO_2 is formed in chain-breaking reactions, i.e., reactions which remove radicals from the mixture, thereby inhibiting product formation.

Relative reduction in induction time.- Figures 22 to 25 illustrate the relative reduction in induction time as a function of mole fraction of initial radical at pressures of 0.5, 1.0, 2.0, and 4.0 atm. These figures show that the effectiveness of O, H, and OH radicals in reducing induction time is inversely related to initial temperature and tends to level out as mole fraction increases. Atomic oxygen is consistently more effective than atomic hydrogen and hydroxyl. Pressure has an effect on the relative reduction in induction time, but it is not consistent. The omission from figure 25 of a relationship for the initial temperature of 1100 K is due to the fact that the induction time for these state conditions is excessive, i.e., beyond 400 μsec, as may be seen in figure 8. Therefore, $\Delta\tau/\tau_0$ was not calculated.

The peculiar relation between $\Delta\tau/\tau_0$ and pressure at various atomic oxygen mole fractions is presented in figure 26. Although the trends show some measure of dependence, the effect of pressure is minor below 2.0 atm. At 4.0 atm the effect is pronounced.

For values of X_O larger than 0.3×10^{-5}, pressure reduces induction time; for X_O less than 0.3×10^{-5}, pressure increases induction time. This phenomenon is presumed to be caused by third-body reactions which involve atomic oxygen. When the initial amount of this radical is present in sufficent quantity, it interacts with other species and thereby enhances reaction. However, when the quantity of atomic oxygen is very small, the pressure dependent reaction 6 becomes predominant and inhibits the reaction.

The next parametric investigation was the effect of ϕ on $\Delta\tau/\tau_0$ for a family of values of X_O. The results are displayed at two pressures, 1.0 and 4.0 atm, in figures 27 and 28, respectively. The variation of $\Delta\tau/\tau_0$ with ϕ is not particularly remarkable; this is as expected, since even at stoichiometric proportions the mass fraction of H_2 is much less than for N_2 or O_2. In figures 27 and 28 it is noted that the curve for $X_O = 10^{-6}$ does show an inverse relationship of $\Delta\tau/\tau_0$ with ϕ.

The variation of $\Delta\tau/\tau_0$ with T_1 for a family of X_O is depicted by figure 29. As is roughly indicated in figures 5 to 9, $\Delta\tau/\tau_0$ is inversely proportional to T_1, also, from figure 12 and figures 22 to 26, it can be seen that increasing values of X_O correspond to increasing values of $\Delta\tau/\tau_0$. An attempt was made to determine a parametric expression from the information generated by the computations. The plan was to find coefficients of X_O, X_H, and X_{OH} which would correlate the curves of $\Delta\tau/\tau_0$ versus radical species mole fraction into a single line for each T_1. Next would be correlation of initial temperatures by finding the required function of T_1. Finally, the effects of p and ϕ would be included.

An abscissa transformation performed for the curves for X_H and X_{OH} relative to the curve for X_O on each of figures 22 to 25; it was determined that H and OH were approximately 60 percent as effective as O in increasing $\Delta\tau/\tau_0$. Therefore, an effective mole fraction was defined as

$$X_e = X_O + 0.6(X_H + X_{OH})$$

Since the 60-percent approximate effectiveness appeared valid for 0.5, 1.0, and 2.0 atm, the effects of pressure were considered masked. It should be noted that the 60-percent value applies to the set of rate constants used.

Merging of the initial temperature family of curves into a single expression was not successful, although curves expressing $\Delta\tau/\tau_0$ versus X_e were found for the intermediate values of $T_1 = 1300$ K and 1400 K by linear interpolation between $T_1 = 1200$ K and 1500 K. Figure 30 shows a family of T_1 curves, including the interpolated ones of 1300 K and 1400 K.

It is noted that the lack of accuracy of rate constants and third-body efficiencies form a limit to the accuracy of this analysis. As new experimental values are deter-

mined, they may easily be substituted into the program. For example, the rate constants for reactions 2 and 3 were changed and are listed in table 2 as k_{2A} and k_{3A}. Consider two mixtures at an initial temperature of 1200 K, a pressure of 1 atm, and an equivalence ratio of unity, one mixture without initial free radicals and one mixture with an initial mole fraction of 10^{-4} of atomic oxygen. The rate constant k_{2A} gave induction times of 38 μsec and 14.5 μsec for the two mixtures, respectively, and the rate constant k_{3A} gave induction times of 41.86 μsec and 16.1 μsec for the two mixtures, respectively, compared with the values of 40.4 μsec and 15.32 μsec obtained using k_2 and k_3. Also, the relative reductions in induction time for k_{2A} and k_{3A} were found to be 0.618 and 0.615, respectively, compared with 0.621 using k_2 and k_3.

Before this investigation was completed, an updated experimental value for the rate of the twelfth reaction $(H_2 + O_2 = OH + OH)$ became available from reference 16. The newer one (designated 12A) was used in the computation of induction time. Figure 31 is a comparison of induction time relative to initial temperature for computations using k_{12} and k_{12A}. The use of k_{12A} reduces induction time, but only very slightly.

In order to compare the criteria for the induction time of references 2 and 5, the concentration of hydroxyl radical was calculated for two mixtures. Both mixtures had an initial temperature of 1200 K, pressure of 1 atm, and an equivalence ratio of unity. However, one mixture initially contained 10^{-4} mole fraction of atomic oxygen. When the mixtures had experienced 5 percent of the equilibrium temperature rise (ref. 5), the hydroxyl concentration was found to be 1.4×10^{-5} mole per liter and 1.8×10^{-5} mole per liter for the mixtures without and with initial atomic oxygen, respectively. This was believed to be a reasonable agreement with the criterion of reference 2. Also, the criteria for references 3 and 5 were compared. Using the same mixtures as before, it was found that maximum atomic hydrogen concentration, i.e., before beginning of third-body recombination (ref. 3), occurred at 48 μsec and 23 μsec for the mixtures without and with atomic oxygen, respectively. This compared fairly well with 40.4 μsec and 15.32 μsec for the induction time as defined by the criterion of reference 5 and used in the present paper.

Reaction time. - The final portion of this investigation considered the effects of trace amounts of O, H, and OH radicals on reaction time. The reaction time was found to be unaffected. Figure 32 is a map of reaction time as a function of the reciprocal of mean temperature for intersecting families of pressure and initial temperature. The mean temperature was used in order to obtain a direct comparison to reference 5 as shown in the figure. Reference 5 indicated a correlation given by

$$\log \tau_r p^{1.6} = \frac{3480}{T_m} + 0.040$$

Several of the rate constants are different from those used in reference 5, and the third-body efficiency of reaction 8 is four times as great. The value of third-body efficiency did not affect the induction time but was inversely related to the total time, thereby changing the reaction time. Thus, the accuracy of the analysis is limited by the accuracy of the rate constants and the third-body efficiencies. The missing regions of the graph represent those low initial temperature, high pressure regimes for which the induction times were too large to be calculated. The parallelism of the isobars on the small semilogarithmic plot suggested that they could be condensed to a single curve. The curve obtained by correlation was of the form

$$\log \tau_r p^{1.641} = \frac{2877}{T_m} + 0.47$$

which plots coincident with the curve $p = 1.0$ atm and the ordinate expressed as $\tau_r p^{1.641}$, μsec-(atm)$^{1.641}$.

A more convenient independent variable for reaction time is initial temperature. This relationship is shown by figure 33. Also shown in this figure is a comparison from reference 18. The correlation given by reference 18 is

$$\tau_r = 10^5 p^{1.7} e^{1.12 \frac{T_1}{1000}}$$

which can also be expressed as

$$\log \tau_r p^{1.7} = -0.0004486 T_1 + 2.021$$

This correlation determined in the present analysis was

$$\log \tau_r p^{1.641} = -0.000415 T_1 + 2.427$$

CONCLUDING REMARKS

Quantitative analytical results have been computed which show that small amounts of atomic oxygen, atomic hydrogen, and hydroxyl radicals reduce induction time of hydrogen-air mixtures undergoing autoignition.

The peak of the reaction chain-breaking species, hydroperoxyl, is especially definitive and seems to be a logical criterion for defining induction time. For mixtures either containing or not containing initial free radicals, the peak of hydroperoxyl occurs consistently near the time of 5-percent fractional temperature rise.

Relative reduction in induction time is found to be a convenient index to measure the comparative effectiveness of the different initial free radicals, as well as their concentration. Atomic oxygen was consistently more effective than atomic hydrogen or

hydroxyl. On the average, both atomic hydrogen and hydroxyl were found to be 60 percent as effective as atomic oxygen.

The equilibrium temperature was not affected by the presence of small amounts of radicals. Evidently, this was due to the fact that the initial and equilibrium composition and enthalpy values were not significantly changed.

The addition of small amounts of radicals to the initial reacting gases did not affect the reaction time (the time between 5 and 95 percent of the equilibrium temperature).

The accuracy of this analysis was limited by the accuracy of available reaction-rate constants and third-body efficiencies. Both of these quantities are easily changed in the chemical kinetics computer program that was used.

Langley Research Center,
National Aeronautics and Space Administration,
Hampton, Va., September 19, 1974.

REFERENCES

1. Engineering Staff: Hypersonic Research Engine Project – Phase IIA. Combustor Program. Second Interim Technical Data Report. Rep. No. AP-67-2535 (Contract No. NAS 1-6666), AiResearch Manufacturing Co., Garrett Corp., Sept. 1, 1967. (Available as NASA CR-66956.)

2. Schott, G. L.; and Kinsey, J. L.: Kinetic Studies of Hydroxyl Radicals in Shock Waves. II. Induction Times in the Hydrogen-Oxygen Reaction. J. Chem. Phys., vol. 29, no. 5, Nov. 1958, pp. 1177-1182.

3. Brokaw, Richard S.: Analytic Solutions to the Ignition Kinetics of the Hydrogen-Oxygen Reaction. Tenth Symposium (International) on Combustion, Combust. Inst., 1965, pp. 269-278.

4. Belles, F. E.; and Lauver, M. R.: Effects of Concentration and of Vibrational Relaxation on the Induction Period of the H_2-O_2 Reaction. Tenth Symposium (International) on Combustion, Combust. Inst., 1965, pp. 285-293.

5. Erickson, Wayne D.; and Klich, George F.: Analytical Chemical Study of the Effect of Carbon Dioxide and Water Vapor on Hydrogen-Air Constant-Pressure Combustion. NASA TN D-5768, 1970.

6. Anon.: U.S. Standard Atmosphere, 1962. NASA, U.S. Air Force, and U.S. Weather Bur., Dec. 1962.

7. Dixon-Lewis, G.; Wilson, W. E.; and Westenberg, A. A.: Studies of Hydroxyl Radical Kinetics by Quantitative ESR. J. Chem. Phys., vol. 44, no. 8, Apr. 15, 1966, pp. 2877-2884.

8. Jachimowski, Casimir J.; and Houghton, William M.: Shock-Tube Study of the Induction-Period Kinetics of the Hydrogen-Oxygen Reaction. Combust. & Flame, vol. 15, no. 2, Oct. 1970, pp. 125-132.

9. Baulch, D. L.; Drysdale, D. D.; and Lloyd, A. C.: Critical Evaluation of Rate Data for Homogeneous, Gas-Phase Reactions of Interest in High-Temperature Systems. High Temperature Reaction Rate Data, No. 3, Univ. of Leeds (England), Apr. 1969.

10. Wong, E. L.; and Potter, A. E.: Mass-Spectrometric Investigation of the Reactions of O-Atoms With H_2 and NH_3. J. Chem. Phys., vol. 43, no. 9, Nov. 1, 1965, pp. 3371-3382.

11. Myerson, A. L.; Watt, W. S.; and Joseph, P. J.: Atom Formation Rated Behind Shock Waves in Hydrogen and the Effect of Added Oxygen. Rep. No. AD-1689-A-7 (Contract No. NASr-109), Cornell Aeronaut. Lab., Inc., Nov. 1966.

12. Kiefer, John H.; and Lutz, Robert W.: Recombination of Oxygen Atoms at High Temperatures as Measured by Shock-Tube Densitometry. J. Chem. Phys., vol. 42, no. 5, Mar. 1, 1965, pp. 1709-1714.

13. Kaskan, W. E.; and Browne, W. G.: Kinetics of the $H_2/CO/O_2$ System. R64SD37 (Contract AF 04(694)-222), Missile Space Div., Gen. Elec. Co., July 1964.

14. Gutman, David, Hardwidge, Edward A.; Dougherty, Frank A.; and Lutz, Robert W.: Shock-Tube Study of the Recombination Rate of Hydrogen Atoms With Oxygen Molecules. J. Chem. Phys., vol. 47, no. 11, Dec. 1967.

15. Baldwin, R. R.; and Bratton, D.: Homogeneous Gas-Phase Decomposition of Hydrogen Peroxide. Eighth Symposium (International) on Combustion, Williams & Wilkins Co., 1962, pp. 110-119.

16. Jachimowski, Casimir J.; and Houghton, William M.: Shock-Tube Study of the Initiation Process in the Hydrogen-Oxygen Reaction. Combust. & Flame, vol. 17, no. 1, Aug. 1971, pp. 25-30.

17. Lewis, Bernard; and Von Elbe, Guenther: Combustion, Flames and Explosions of Gases. Second ed., Academic Press, Inc., 1961, pp. 29-85.

18. Pergament, Harold S.: A Theoretical Analysis of Non-Equilibrium Hydrogen-Air Reactions in Flow Systems. [Preprint] 63113, American Inst. Aeronaut. & Astronaut., Apr. 1963.

TABLE 1.- COMPOSITION OF BASELINE MIXTURES

IN MASS FRACTIONS

ϕ	Y_{N_2}	Y_{O_2}	Y_{H_2}
0	0.768	0.232	0
.2	.7635343	.230651	.0058124
.6	.7547621	.2280011	.0172367
1.0	.7462104	.2254107	.0284017
1.2	.7419728	.2241376	.0338896

TABLE 2.- REACTION RATE CONSTANTS

j	Reaction	Reaction rate constant (a)	Source
1	$OH + H_2 \underset{k_{-1}}{\overset{k_1}{\rightleftharpoons}} H_2O + H$	$k_1 = 2.3 \times 10^{13} \exp(-5200/RT)$	Dixon-Lewis, Wilson, and Westenberg (ref. 7)
2	$H + O_2 \underset{k_{-2}}{\overset{k_2}{\rightleftharpoons}} OH + O$	$k_2 = 9.9 \times 10^{13} \exp(-15\ 020/RT)$	Jachimowski and Houghton (ref. 8)
2A	$H + O_2 \underset{k_{-2A}}{\overset{k_{2A}}{\rightleftharpoons}} OH + O$	$k_{2A} = 2.24 \times 10^{14} \exp(-16\ 800/RT)$	(ref. 9)
3	$O + H_2 \underset{k_{-3}}{\overset{k_3}{\rightleftharpoons}} OH + H$	$k_3 = 7.5 \times 10^{13} \exp(-11\ 100/RT)$	Jachimowski and Houghton (ref. 8)
3A	$O + H_2 \underset{k_{-3A}}{\overset{k_{3A}}{\rightleftharpoons}} OH + H$	$k_{3A} = 4.3 \times 10^{13} \exp(-10\ 200/RT)$	Wong and Potter (ref. 10)
4	$OH + OH \underset{k_{-4}}{\overset{k_4}{\rightleftharpoons}} H_2O + O$	$k_4 = 1.55 \times 10^{12} \exp(1000/RT)$	Dixon-Lewis, Wilson, and Westenberg (ref. 7)
5	$H + H + M \underset{k_{-5}}{\overset{k_5}{\rightleftharpoons}} H_2 + M$	$k_{5,Ar}\ 8.5632 \times 10^{11} T^{0.45} \exp(11\ 590/RT)$	Myerson, Watt, and Joseph (ref. 11)
6	$O + O + M \underset{k_{-6}}{\overset{k_6}{\rightleftharpoons}} O_2 + M$	$k_{6,O_2} = 8.2 \times 10^{18} T^{-1.22}$	Kiefer and Lutz (ref. 12)
7	$O + H + M \underset{k_{-7}}{\overset{k_7}{\rightleftharpoons}} OH + M$	$k_{7,M} = 6.0 \times 10^{14}$	Kaskan and Browne (ref. 13)
8	$H + OH + M \underset{k_{-8}}{\overset{k_8}{\rightleftharpoons}} H_2O + M$	$k_{8,M} = 4.5 \times 10^{21} T^{-1.5}$	Kaskan and Browne (ref. 13)
9	$H + O_2 + M \underset{k_{-9}}{\overset{k_9}{\rightleftharpoons}} HO_2 + M$	$k_{9,Ar} = 2.0 \times 10^{15} \exp(870/RT)$	Gutman, Hardwidge, Doughert, and Lutz (ref. 14)
10	$HO_2 + H_2 \underset{k_{-10}}{\overset{k_{10}}{\rightleftharpoons}} H_2O_2 + H$	$k_{10} = 9.6 \times 10^{12} \exp(-24\ 000/RT)$	(ref. 9)
11	$H_2O_2 + M \underset{k_{-11}}{\overset{k_{11}}{\rightleftharpoons}} OH + OH + M$	$k_{11,N_2} = 1.7 \times 10^{17} \exp(-46\ 300/RT)$	Baldwin and Bratton (ref. 15)
12	$H_2 + O_2 \underset{k_{-12}}{\overset{k_{12}}{\rightleftharpoons}} OH + OH$	$k_{12} = 1.05 \times 10^{13} \exp(-48\ 080/RT)$	Jachimowski and Houghton (preliminary to ref. 16)
12A	$H_2 + O_2 \underset{k_{-12A}}{\overset{k_{12A}}{\rightleftharpoons}} OH + OH$	$k_{12A} = 1.70 \times 10^{13} \exp(-48\ 150/RT)$	Jachimowski and Houghton (ref. 16)

[a]All reactions have units of $cm^3/mol\text{-}sec$ except reactions 5 to 8, 10, and 12 which have units of $cm^6/mol^2\text{-}sec$; activation energies are expressed in units of cal/mol (1 cal/mol = 4.184 J/mol).

TABLE 3.- INDUCTION-TIME FUNCTIONS

ϕ	T_1	p	X_O	X_H	X_{OH}	τ	τ/τ_o	$\Delta\tau/\tau_o$
0.2	1100	1.0	0	0	0	99.92	1.000	0.000
			10^{-6}	0	0	60.80	.608	.392
			0	10^{-6}	0	63.37	.634	.366
			0	0	10^{-6}	63.91	.640	.360
			10^{-5}	0	0	44.14	.442	.558
			0	10^{-5}	0	46.72	.468	.532
			0	0	10^{-5}	47.26	.473	.527
			10^{-4}	0	0	27.64	.277	.723
			0	10^{-4}	0	30.66	.307	.693
			0	0	10^{-4}	30.75	.308	.692
0.2	1200	1.0	0	0	0	49.46	1.000	0.000
			10^{-6}	0	0	33.94	.686	.314
			0	10^{-6}	0	34.80	.704	.296
			0	0	10^{-6}	35.22	.712	.288
			10^{-5}	0	0	25.64	.518	.482
			0	10^{-5}	0	26.48	.535	.465
			0	0	10^{-5}	26.86	.543	.457
			10^{-4}	0	0	17.30	.350	.650
			0	10^{-4}	0	18.13	.367	.633
			0	0	10^{-4}	18.56	.375	.625
			10^{-5}	10^{-5}	0	23.50	.475	.525
			10^{-5}	0	10^{-5}	23.70	.479	.521
			0	10^{-5}	10^{-5}	24.18	.488	.511
			10^{-5}	10^{-5}	10^{-5}	22.34	.452	.548
			10^{-5}	0	10^{-6}	25.38	.513	.487
0.2	1200	4.0	0	0	0	31.73	1.000	0.000
			10^{-6}	0	0	21.18	.668	.332
			0	10^{-6}	0	22.90	.722	.278
			0	0	10^{-6}	22.94	.722	.277
			10^{-5}	0	0	13.99	.441	.559
			0	10^{-5}	0	15.63	.492	.508
			0	0	10^{-5}	15.90	.501	.499
			10^{-4}	0	0	7.09	.223	.777
			0	10^{-4}	0	8.62	.272	.728
			0	0	10^{-4}	8.70	.274	.726

TABLE 3.- INDUCTION-TIME FUNCTIONS – Continued

ϕ	T_1	p	X_O	X_H	X_{OH}	τ	τ/τ_O	$\Delta\tau/\tau_O$
0.2	1500	1.0	0	0	0	16.90	1.000	0.000
			10^{-6}	0	0	14.62	.865	.135
			0	10^{-6}	0	14.64	.066	.154
			0	0	10^{-6}	14.98	.886	.114
			10^{-5}	0	0	11.87	.702	.298
			0	10^{-5}	0	11.94	.707	.293
			0	0	10^{-5}	12.25	.725	.275
			10^{-4}	0	0	8.81	.521	.479
			0	10^{-4}	0	8.94	.530	.471
			0	0	10^{-4}	9.26	.548	.452
0.6	1100	1.0	0	0	0	86.50	1.000	0.000
			10^{-6}	0	0	55.58	.643	.357
			0	10^{-6}	0	58.85	.680	.320
			0	0	10^{-6}	59.10	.683	.317
			10^{-5}	0	0	40.61	.464	.531
			0	10^{-5}	0	44.25	.512	.488
			0	0	10^{-5}	44.49	.514	.486
			10^{-4}	0	0	26.16	.302	.698
			0	10^{-4}	0	29.28	.338	.662
			0	0	10^{-4}	29.92	.346	.654
0.6	1200	0.5	0	0	0	74.25	1.000	0.000
			10^{-6}	0	0	53.90	.726	.274
			0	10^{-6}	0	55.95	.754	.246
			0	0	10^{-6}	56.44	.760	.240
			10^{-5}	0	0	41.86	.564	.436
			0	10^{-5}	0	44.27	.596	.404
			0	0	10^{-5}	44.62	.601	.399
			10^{-4}	0	0	29.91	.309	.597
			0	10^{-4}	0	32.19	.434	.566
			0	0	10^{-4}	32.66	.440	.560
0.6	1200	1.0	0	0	0	40.15	1.000	0.000
			10^{-6}	0	0	28.81	.718	.282
			0	10^{-6}	0	30.10	.750	.250
			0	0	10^{-6}	30.35	.760	.244

TABLE 3.- INDUCTION-TIME FUNCTIONS – Continued

ϕ	T_1	p	X_O	X_H	X_{OH}	τ	τ/τ_O	$\Delta\tau/\tau_O$
0.6	1200	1.0	10^{-5}	0	0	22.00	0.547	0.452
			0	10^{-5}	0	23.42	.583	.417
			0	0	10^{-5}	23.62	.588	.412
			10^{-4}	0	0	15.20	.379	.621
			0	10^{-4}	0	16.46	.410	.590
			0	0	10^{-4}	16.75	.417	.583
			10^{-5}	10^{-5}	10^{-5}	19.64	.489	.511
0.6	1200	4.0	0	0	0	34.30	1.000	0.000
			10^{-6}	0	0	25.00	.729	.271
			0	10^{-6}	0	27.91	.814	.186
			10^{-5}	0	0	16.14	.471	.529
			0	10^{-5}	0	18.74	.546	.454
			10^{-4}	0	0	8.24	.240	.760
			0	10^{-4}	0	10.20	.297	.703
0.6	1500	1.0	0	0	0	12.08	1.000	0.000
			10^{-6}	0	0	10.74	.889	.111
			0	10^{-6}	0	11.10	.919	.081
			0	0	10^{-6}	11.10	.919	.081
			10^{-5}	0	0	8.64	.716	.284
			0	10^{-5}	0	9.10	.754	.246
			0	0	10^{-5}	9.21	.763	.237
			10^{-4}	0	0	6.60	.547	.453
			0	10^{-4}	0	6.83	.566	.434
			0	0	10^{-4}	7.20	.596	.404
1.0	1100	0.5	0	0	0	139.45	1.000	0.000
			10^{-6}	0	0	92.31	.662	.338
			0	10^{-6}	0	97.56	.700	.300
			0	0	10^{-6}	97.85	.702	.298
			10^{-5}	0	0	70.18	.503	.497
			0	10^{-5}	0	75.57	.542	.458
			0	0	10^{-5}	75.86	.544	.456
			10^{-4}	0	0	48.03	.344	.656
			0	10^{-4}	0	53.20	.381	.618
			0	0	10^{-4}	53.55	.384	.616

TABLE 3.- INDUCTION-TIME FUNCTIONS – Continued

ϕ	T_1	p	X_O	X_H	X_{OH}	τ	τ/τ_O	$\Delta\tau/\tau_O$
1.0	1100	0.5	10^{-5}	10^{-5}	0	65.75	0.471	0.529
			10^{-5}	0	10^{-5}	65.80	.472	.528
			0	10^{-5}	10^{-5}	68.75	.493	.507
			10^{-5}	10^{-5}	10^{-5}	62.92	.451	.549
			10^{-5}	0	10^{-6}	69.60	.499	.501
			10^{-7}	0	0	113.92	.814	.183
			10^{-3}	0	0	26.50	.190	.810
1.0	1100	1.0	0	0	0	92.30	1.000	0.000
			10^{-6}	0	0	60.00	.650	.350
			0	10^{-6}	0	64.20	.696	.304
			0	0	10^{-6}	64.29	.697	.303
			10^{-5}	0	0	44.00	.477	.523
			0	10^{-5}	0	48.43	.525	.475
			0	0	10^{-5}	48.25	.523	.477
			10^{-4}	0	0	28.13	.305	.695
			0	10^{-4}	0	32.50	.352	.648
			0	0	10^{-4}	32.33	.350	.650
			10^{-5}	10^{-5}	0	41.10	.445	.555
			10^{-5}	0	10^{-5}	41.20	.446	.554
			0	10^{-5}	10^{-5}	43.70	.473	.527
			10^{-5}	0	10^{-6}	43.66	.473	.525
			10^{-7}	0	0	75.68	.820	.180
			10^{-3}	0	0	13.55	.147	.853
1.0	1100	2.0	0	0	0	206.85	1.000	0.000
			10^{-6}	0	0	134.00	.648	.352
			0	10^{-6}	0	151.00	.730	.270
			0	0	10^{-6}	151.08	.730	.270
			10^{-5}	0	0	75.90	.367	.633
			0	10^{-5}	0	92.55	.447	.553
			0	0	10^{-5}	92.32	.447	.554
			10^{-4}	0	0	31.60	.153	.847
			0	10^{-4}	0	42.48	.205	.795
			0	0	10^{-4}	42.35	.205	.795
			10^{-5}	10^{-5}	0	66.52	.322	.678
			10^{-5}	0	10^{-5}	66.55	.322	.678

TABLE 3.- INDUCTION-TIME FUNCTIONS – Continued

ϕ	T_1	p	X_O	X_H	X_{OH}	τ	τ/τ_o	$\Delta\tau/\tau_o$
1.0	1200	0.5	0	0	0	74.45	1.000	0.000
			10^{-6}	0	0	54.57	.733	.267
			0	10^{-6}	0	57.17	.768	.232
			0	0	10^{-6}	57.94	.778	.222
			10^{-5}	0	0	42.05	.564	.435
			0	10^{-5}	0	45.16	.607	.393
			0	0	10^{-5}	45.38	.610	.390
			10^{-4}	0	0	30.15	.405	.595
			0	10^{-4}	0	32.94	.442	.558
			0	0	10^{-4}	33.12	.445	.555
			10^{-5}	10^{-5}	0	39.93	.536	.464
			10^{-5}	0	10^{-5}	39.98	.537	.463
			0	10^{-5}	10^{-5}	41.56	.558	.442
			10^{-5}	10^{-5}	10^{-5}	38.30	.514	.486
			10^{-5}	0	10^{-6}	42.11	.566	.434
			10^{-7}	0	0	65.70	.882	.118
			10^{-3}	0	0	18.20	.244	.756
1.0	1200	1.0	0	0	0	40.40	1.000	0.000
			10^{-6}	0	0	29.70	.735	.265
			0	10^{-6}	0	31.22	.773	.227
			0	0	10^{-6}	31.30	.775	.225
			10^{-5}	0	0	22.25	.551	.449
			0	10^{-5}	0	24.30	.601	.399
			0	0	10^{-5}	24.25	.601	.400
			10^{-4}	0	0	15.32	.379	.621
			0	10^{-4}	0	17.32	.429	.571
			0	0	10^{-4}	17.45	.432	.568
			10^{-5}	10^{-5}	0	20.95	.519	.481
			10^{-5}	0	10^{-5}	21.03	.521	.479
			0	10^{-5}	10^{-5}	22.34	.553	.447
			10^{-5}	10^{-5}	10^{-5}	20.25	.501	.499
			10^{-5}	0	10^{-6}	22.34	.553	.447
			10^{-7}	0	0	36.07	.893	.107
			10^{-3}	0	0	8.56	.212	.788

TABLE 3.- INDUCTION-TIME FUNCTIONS – Continued

ϕ	T_1	p	X_O	X_H	X_{OH}	τ	τ/τ_O	$\Delta\tau/\tau_O$
1.0	1200	2.0	0	0	0	26.75	1.000	0.000
			10^{-6}	0	0	19.32	.722	.278
			0	10^{-6}	0	20.50	.766	.234
			0	0	10^{-6}	20.60	.770	.231
			10^{-5}	0	0	14.25	.533	.467
			0	10^{-5}	0	15.52	.580	.419
			0	0	10^{-5}	15.56	.582	.418
			10^{-4}	0	0	9.16	.342	.658
			0	10^{-4}	0	10.48	.392	.608
			0	0	10^{-4}	10.49	.392	.608
			10^{-5}	10^{-5}	0	13.24	.495	.505
			10^{-5}	0	10^{-5}	13.02	.487	.513
			0	10^{-5}	10^{-5}	13.20	.493	.507
			10^{-5}	10^{-5}	10^{-5}	12.57	.470	.530
			10^{-5}	0	10^{-6}	13.30	.497	.502
1.0	1200	4.0	0	0	0	52.84	1.000	0.000
			10^{-6}	0	0	40.33	.763	.237
			0	10^{-6}	0	44.31	.839	.161
			0	0	10^{-6}	44.27	.838	.162
			10^{-5}	0	0	24.57	.465	.535
			0	10^{-5}	0	29.10	.551	.449
			0	0	10^{-5}	29.35	.555	.445
			10^{-4}	0	0	10.15	.192	.808
			0	10^{-4}	0	14.15	.268	.732
			0	0	10^{-4}	14.15	.268	.732
			10^{-5}	10^{-5}	0	22.39	.424	.576
			10^{-5}	0	10^{-5}	21.72	.411	.589
			0	10^{-5}	10^{-5}	24.37	.461	.539
			10^{-5}	10^{-5}	10^{-5}	19.85	.376	.624
			10^{-5}	0	10^{-6}	24.17	.457	.543
1.0	1500	0.5	0	0	0	23.30	1.000	0.000
			10^{-6}	0	0	21.18	.909	.091
			0	10^{-6}	0	21.71	.932	.068
			0	0	10^{-6}	21.83	.937	.063
			10^{-5}	0	0	17.42	.748	.252

TABLE 3.- INDUCTION-TIME FUNCTIONS – Continued

ϕ	T_1	p	X_O	X_H	X_{OH}	τ	τ/τ_o	$\Delta\tau/\tau_o$
1.0	1500	0.5	0	10^{-5}	0	18.18	0.780	0.220
			0	0	10^{-5}	18.38	.789	.211
			10^{-4}	0	0	13.10	.562	.438
			0	10^{-4}	0	13.95	.599	.401
			0	0	0	14.11	.606	.394
			10^{-5}	10^{-5}	10^{-4}	15.30	.657	.343
			10^{-5}	0	10^{-5}	16.56	.711	.289
			0	10^{-5}	10^{-5}	17.02	.730	.269
			10^{-5}	10^{-5}	10^{-5}	15.94	.684	.316
			10^{-5}	0	10^{-6}	17.33	.744	.256
			10^{-7}	0	0	22.76	.977	.023
			10^{-3}	0	0	7.85	.337	.663
1.0	1500	1.0	0	0	0	11.63	1.000	0.000
			10^{-6}	0	0	10.50	.903	.097
			0	10^{-6}	0	10.72	.921	.078
			0	0	10^{-6}	10.77	.925	.074
			10^{-5}	0	0	8.50	.731	.268
			0	10^{-5}	0	8.92	.766	.233
			0	0	10^{-5}	9.00	.773	.226
			10^{-4}	0	0	6.32	.543	.457
			0	10^{-4}	0	6.74	.579	.420
			0	0	10^{-4}	6.83	.587	.413
			10^{-5}	10^{-5}	0	8.04	.691	.308
			10^{-5}	0	10^{-5}	8.09	.695	.305
			0	10^{-5}	10^{-5}	8.33	.715	.284
			10^{-5}	10^{-5}	10^{-5}	7.75	.666	.333
			10^{-5}	0	10^{-6}	8.46	.727	.272
			10^{-7}	0	0	11.41	.981	.019
			10^{-3}	0	0	4.06	.349	.651
1.0	1500	2.0	0	0	0	5.85	1.000	0.000
			10^{-6}	0	0	5.30	.906	.094
			0	10^{-6}	0	5.41	.920	.080
			0	0	10^{-6}	5.41	.920	.080
			10^{-5}	0	0	4.19	.716	.284
			0	10^{-5}	0	4.46	.762	.238

TABLE 3.- INDUCTION-TIME FUNCTION – Concluded

ϕ	T_1	p	X_O	X_H	X_{OH}	τ	τ/τ_o	$\Delta\tau/\tau_o$
1.0	1500	2.0	0	0	10^{-5}	4.51	0.771	0.229
			10^{-4}	0	0	3.08	.513	.487
			0	10^{-4}	0	3.39	.579	.421
			0	0	10^{-4}	3.35	.573	.427
			10^{-5}	10^{-5}	0	3.84	.656	.344
			10^{-5}	0	10^{-5}	4.04	.691	.309
			0	10^{-5}	10^{-5}	4.11	.703	.297
			10^{-5}	10^{-5}	10^{-5}	4.00	.684	.316
			10^{-5}	0	10^{-6}	4.20	.718	.282
1.0	1500	4.0	0	0	0	3.10	1.000	0.000
			10^{-6}	0	0	2.78	.896	.104
			0	10^{-6}	0	2.86	.923	.077
			0	0	10^{-6}	2.88	.928	.072
			10^{-5}	0	0	2.21	.713	.275
			0	10^{-5}	0	2.30	.741	.259
			0	0	10^{-5}	2.37	.765	.240
			10^{-4}	0	0	1.56	.504	.496
			0	10^{-4}	0	1.70	.549	.451
			0	0	10^{-4}	1.72	.556	.444
			10^{-5}	10^{-5}	0	2.12	.683	.317
			10^{-5}	0	10^{-5}	2.14	.690	.310
			0	10^{-5}	10^{-5}	.80	.258	.742
			10^{-5}	10^{-5}	10^{-5}	.70	.226	.774
1.2	1200	1.0	0	0	0	41.72	1.000	0.000
			10^{-6}	0	0	30.64	.734	.266
			0	10^{-6}	0	32.21	.772	.228
			0	0	10^{-6}	32.31	.774	.226
			10^{-5}	0	0	33.32	.557	.443
			0	10^{-5}	0	25.04	.600	.400
			0	0	10^{-5}	25.00	.599	.401
			10^{-4}	0	0	15.94	.382	.618
			0	10^{-4}	0	17.64	.423	.577
			0	0	10^{-4}	17.70	.424	.576

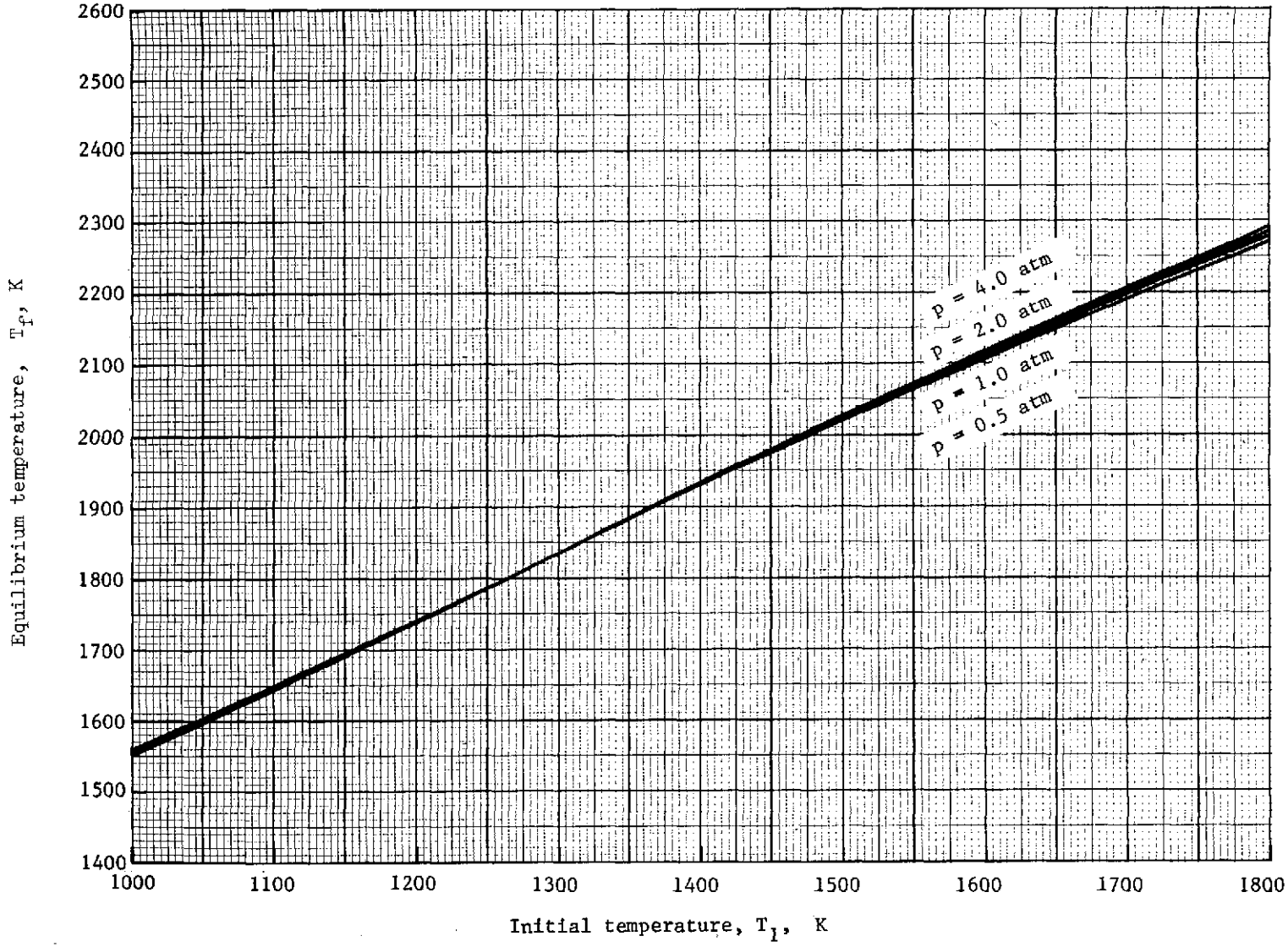

Figure 1.- Equilibrium temperature as a function of initial temperature along isobars for $\phi = 0.2$.

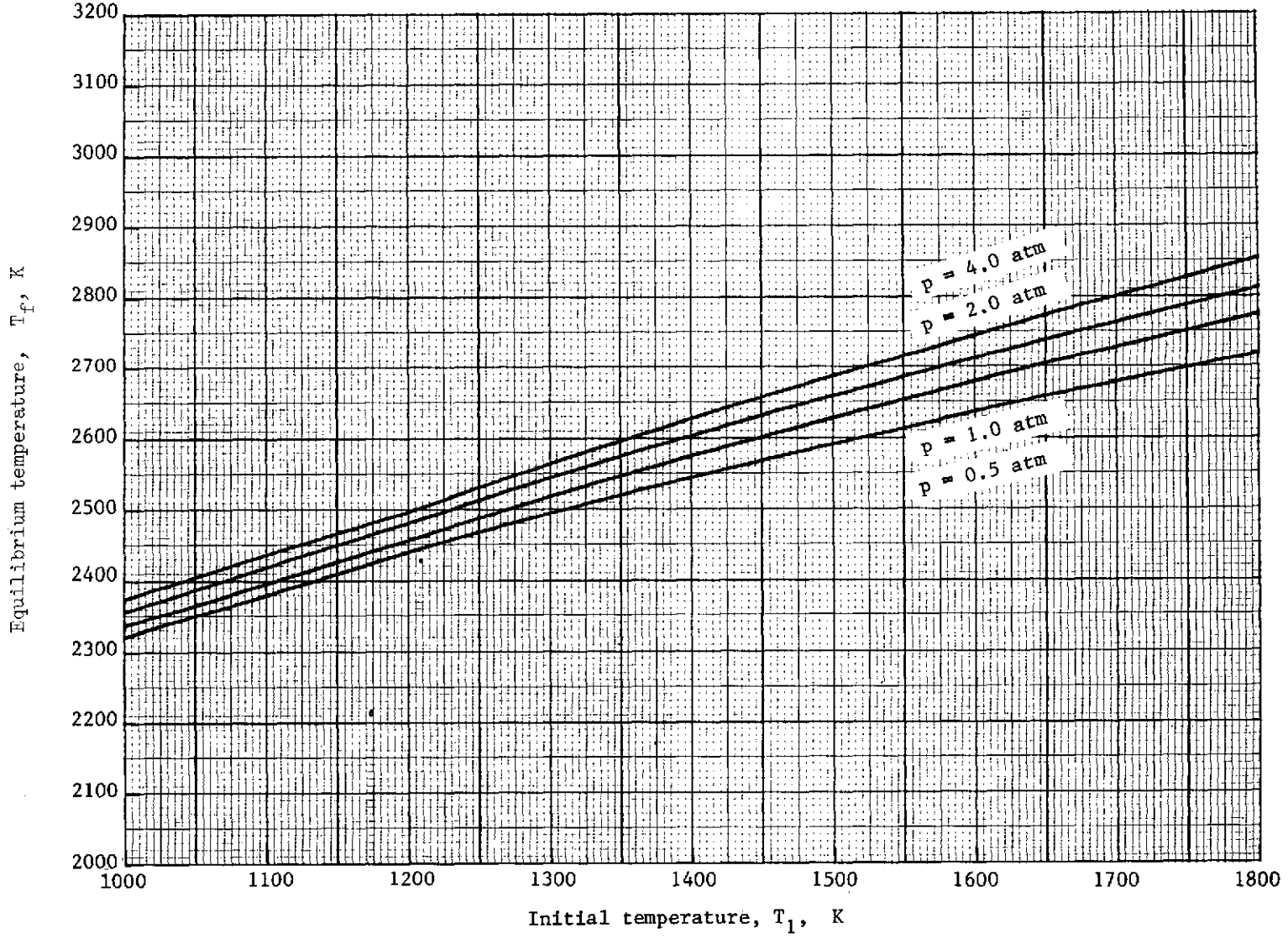

Figure 2.- Equilibrium temperature as a function of initial temperature along isobars for $\phi = 0.6$.

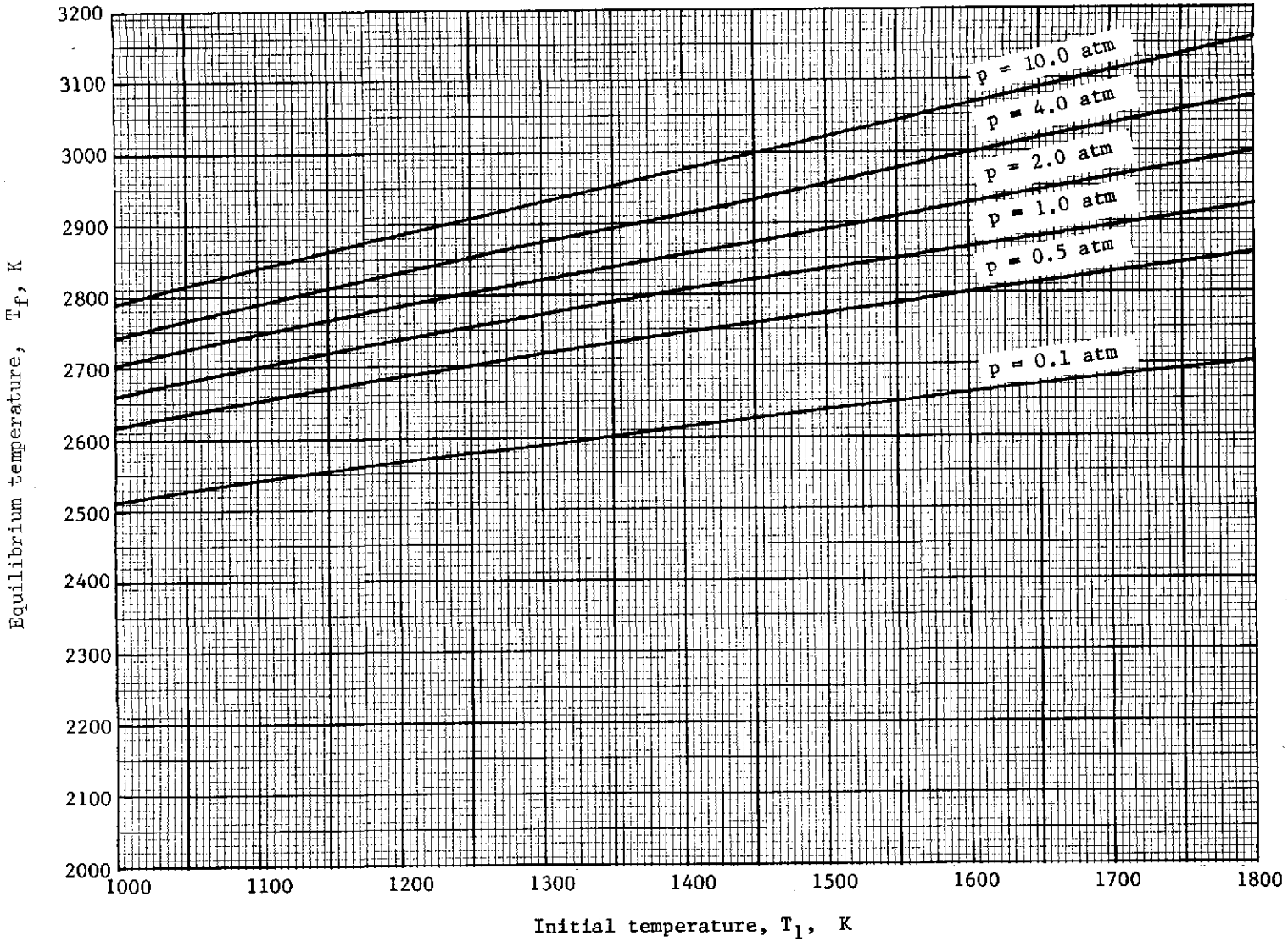

Figure 3.- Equilibrium temperature as a function of initial temperature along isobars for $\phi = 1.0$.

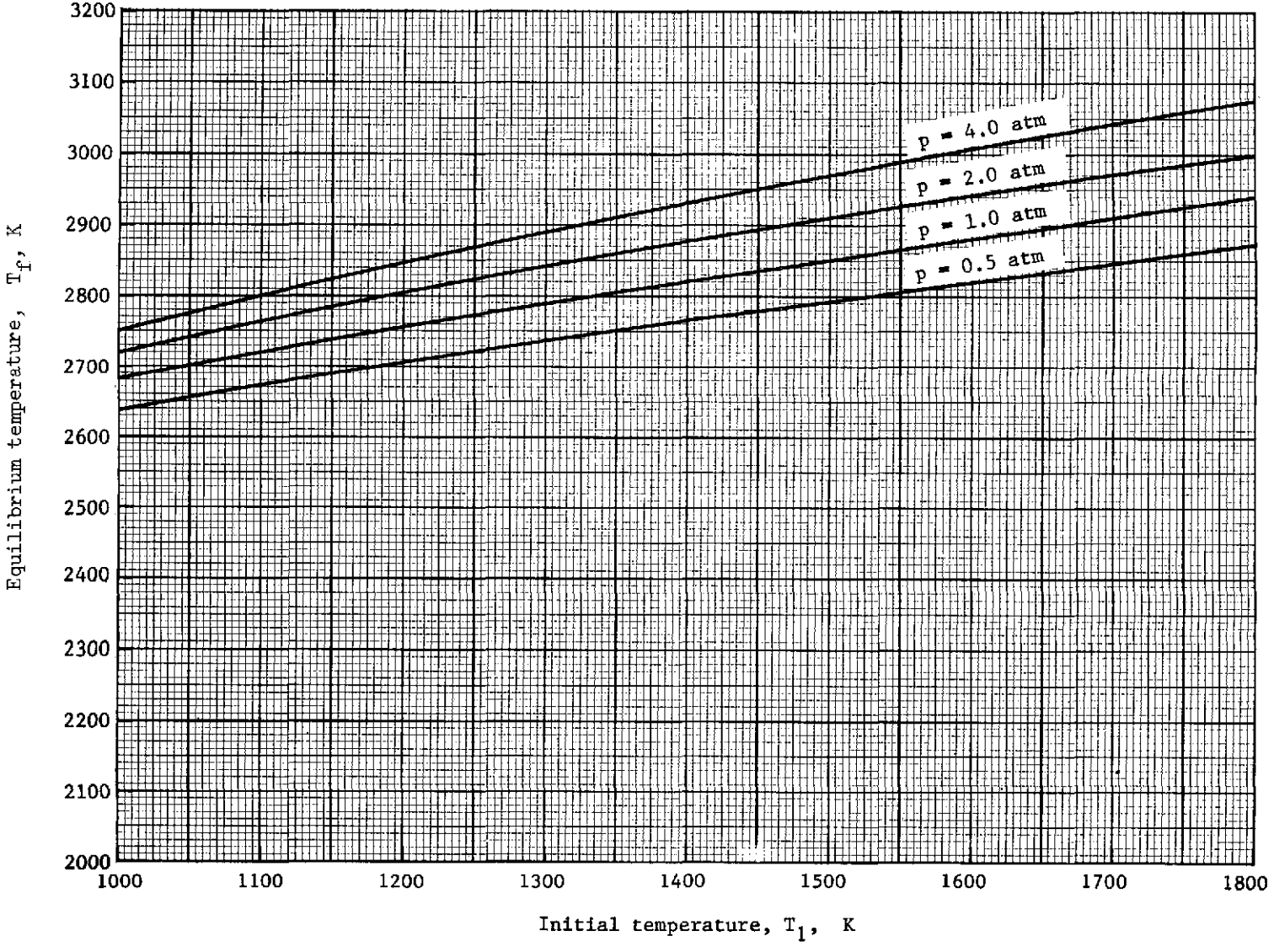

Figure 4.- Equilibrium temperature as a function of initial temperature along isobars for $\phi = 1.2$.

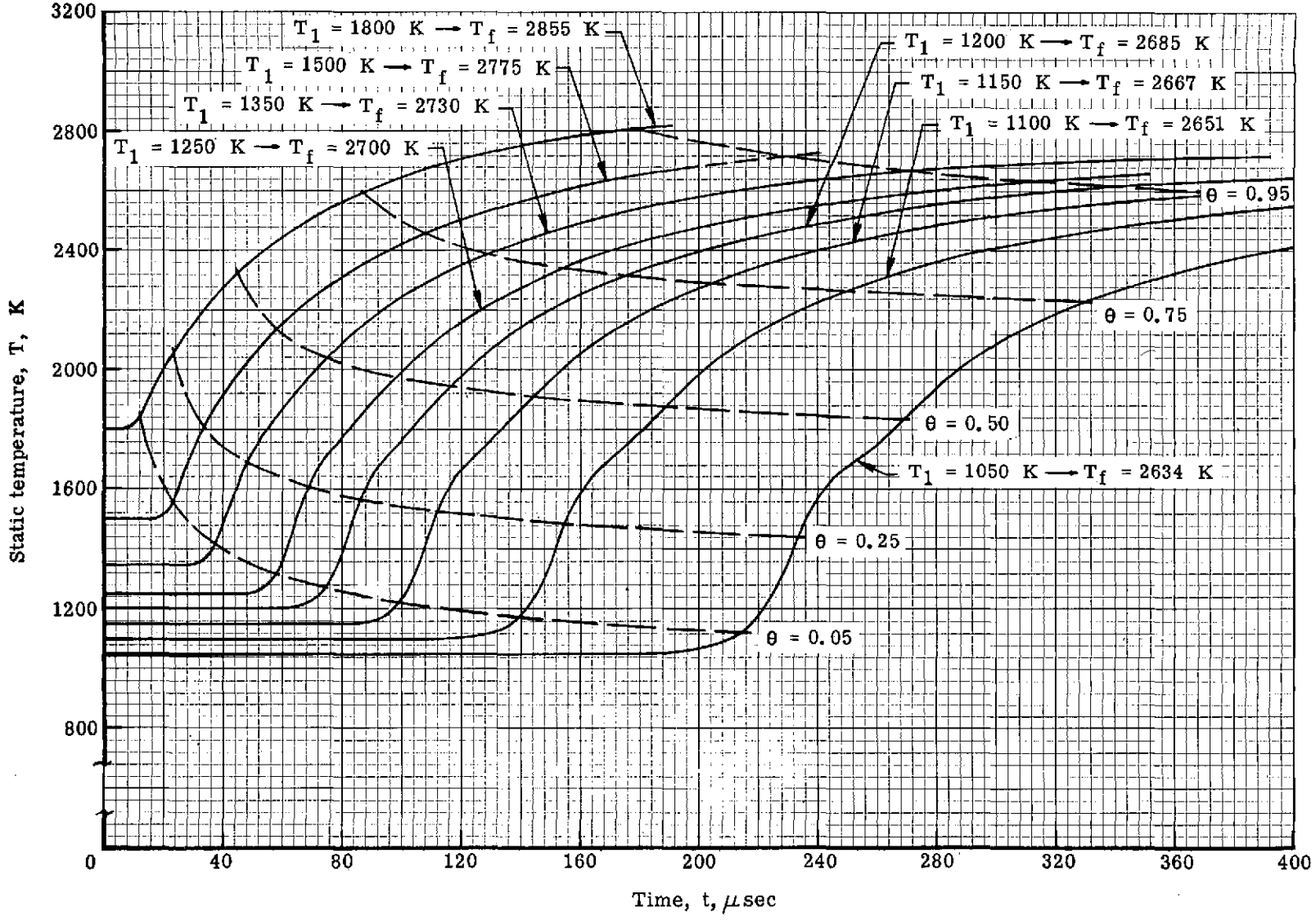

Figure 5.- Isobaric combustion temperature variation with time for p = 0.5 atm and ϕ = 1.0.

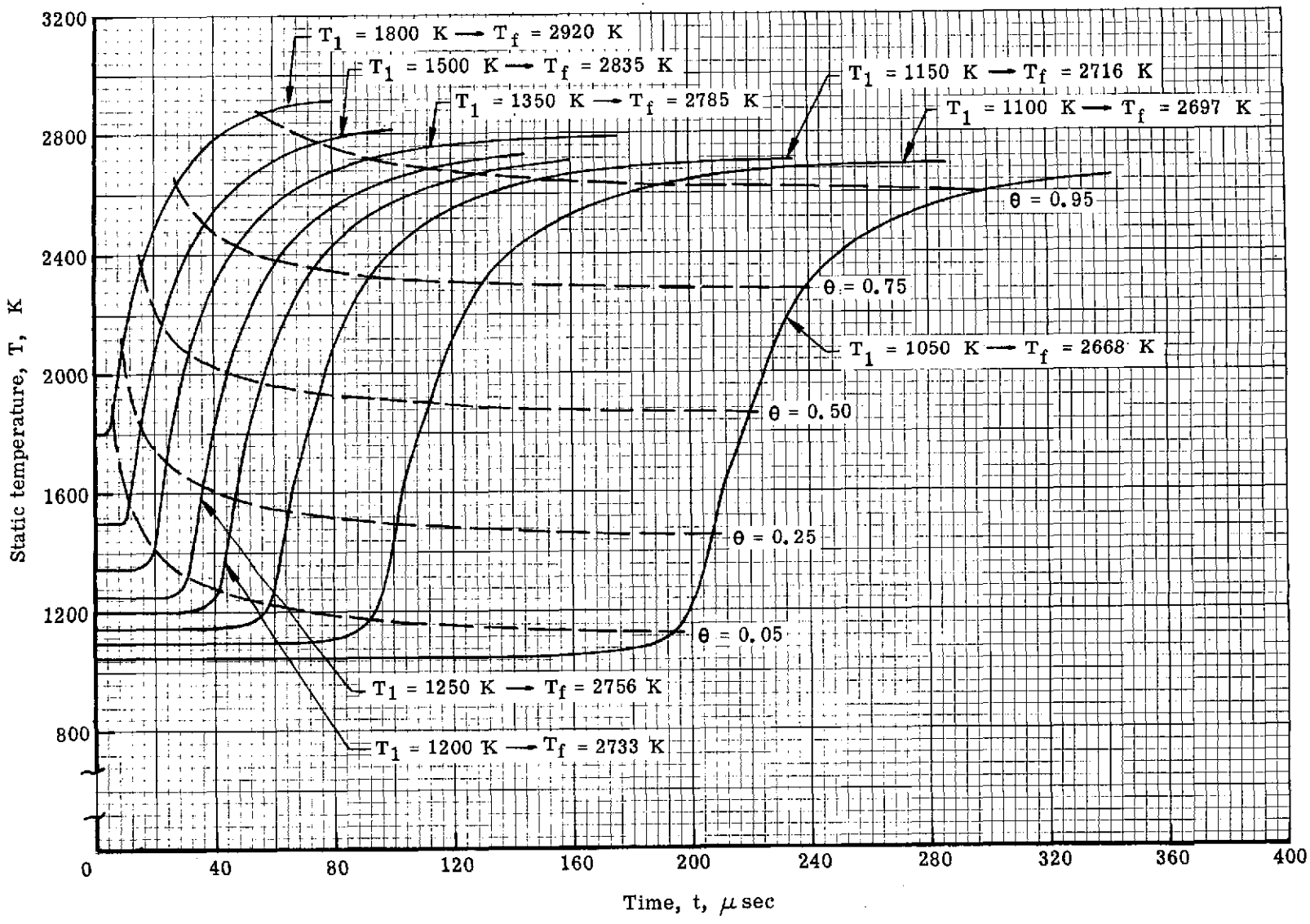

Figure 6.- Isobaric combustion temperature variation with time for p = 1.0 atm and ϕ = 1.0.

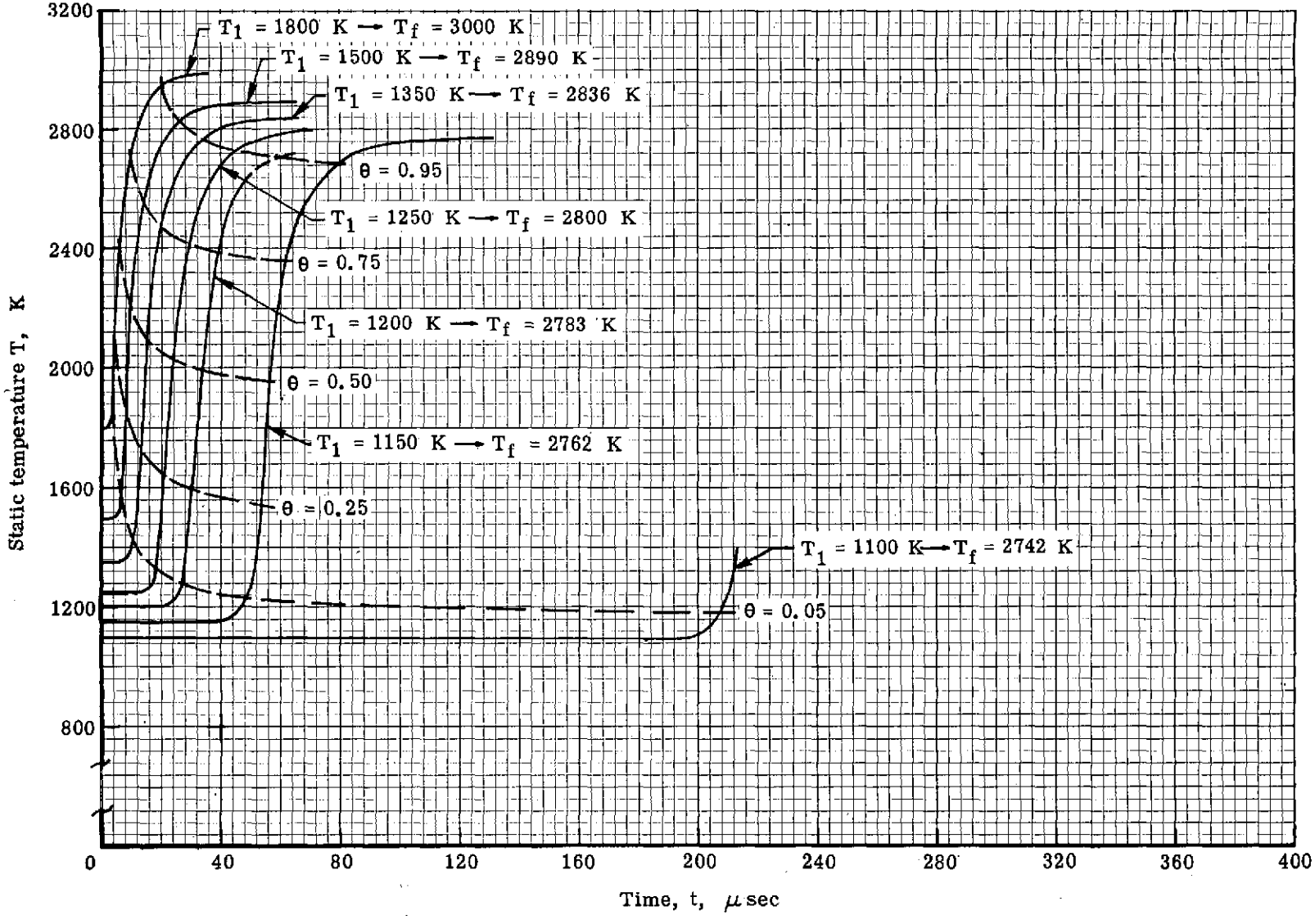

Figure 7.- Isobaric combustion temperature variation with time for p = 2.0 atm and ϕ = 1.0.

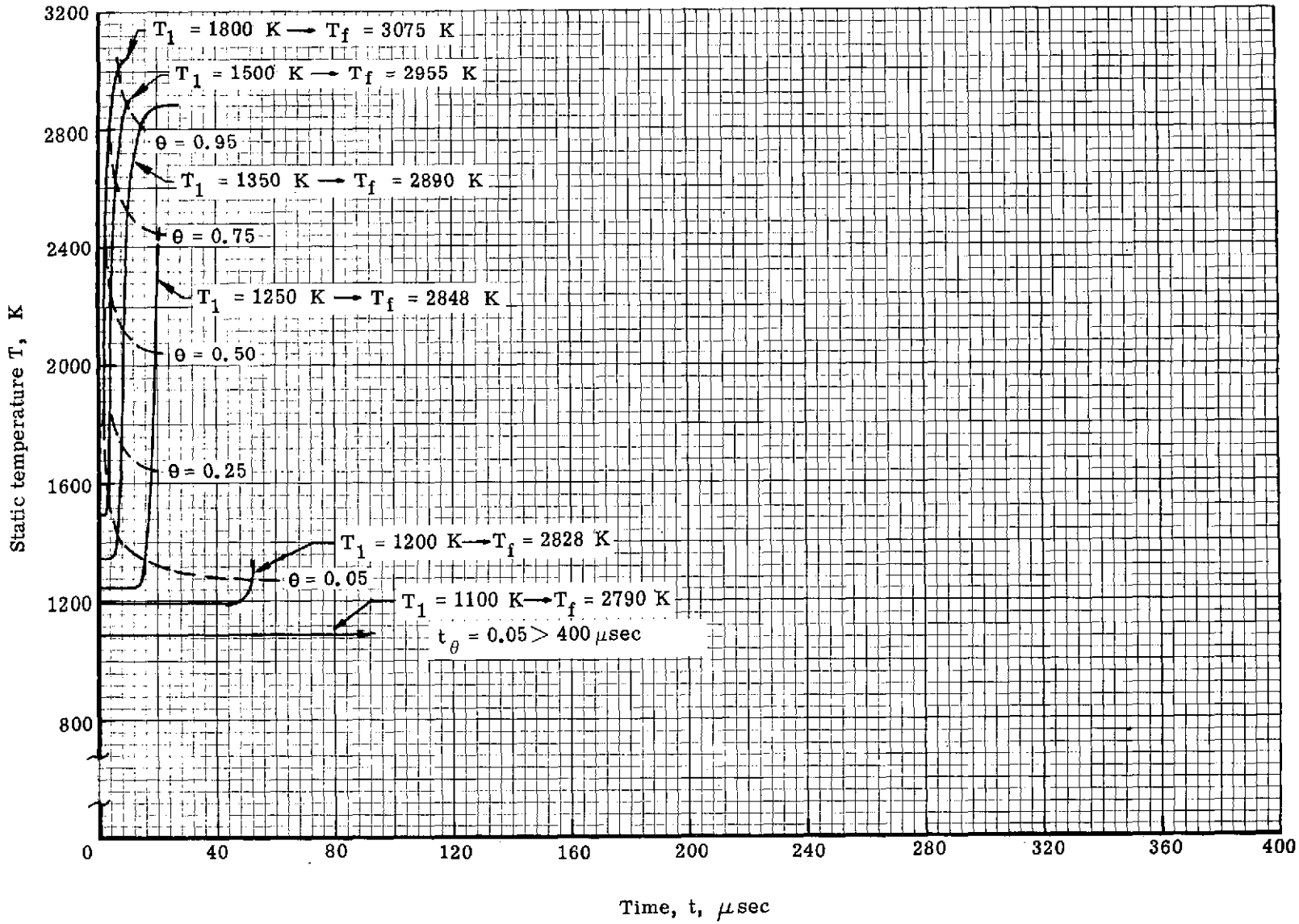

Figure 8.- Isobaric combustion temperature variation with time for p = 4.0 atm and ϕ = 1.0.

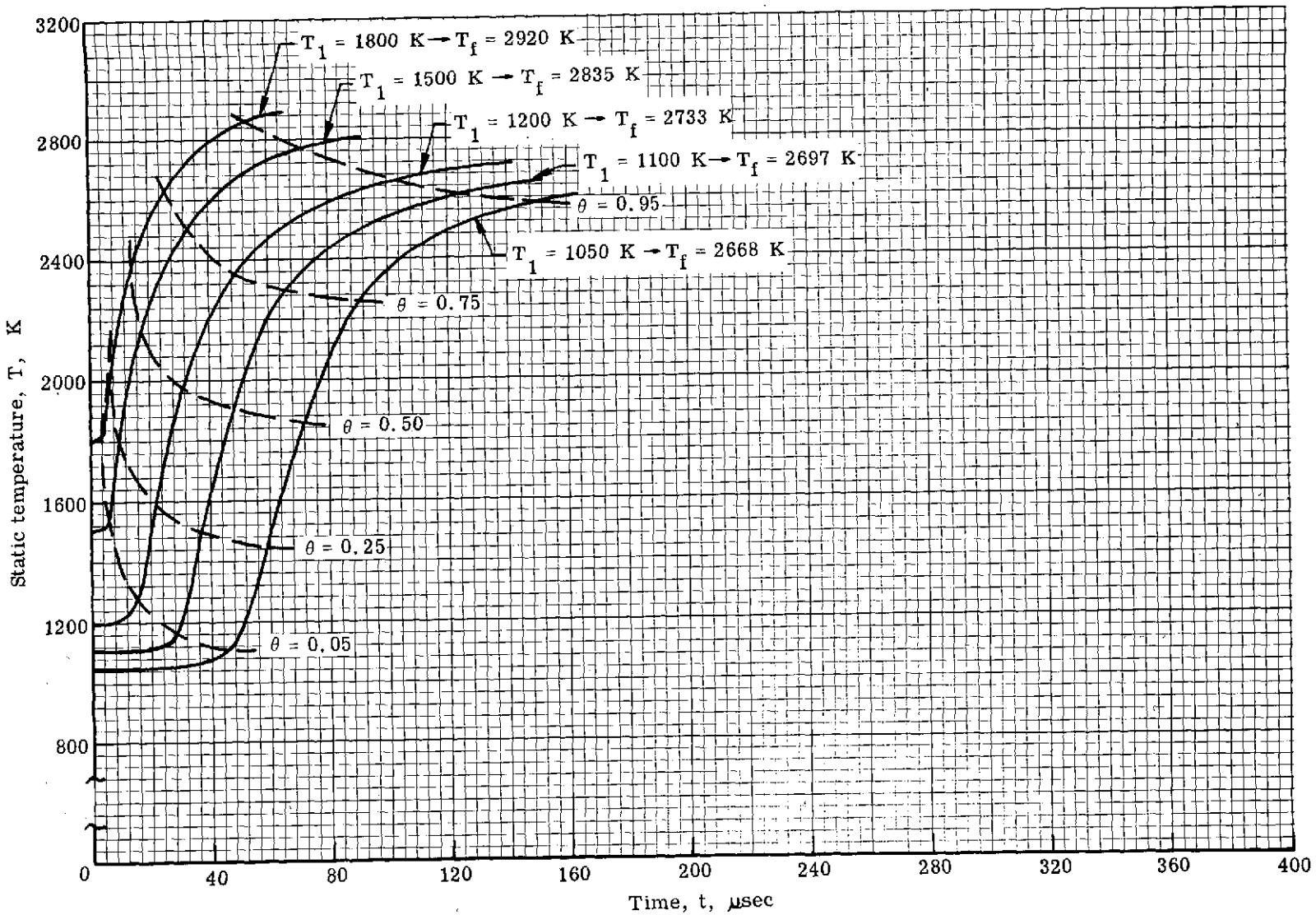

Figure 9.- Isobaric combustion temperature variation with time for $p = 1.0$ atm, $\phi = 1.0$, and $X_O = 10^{-4}$.

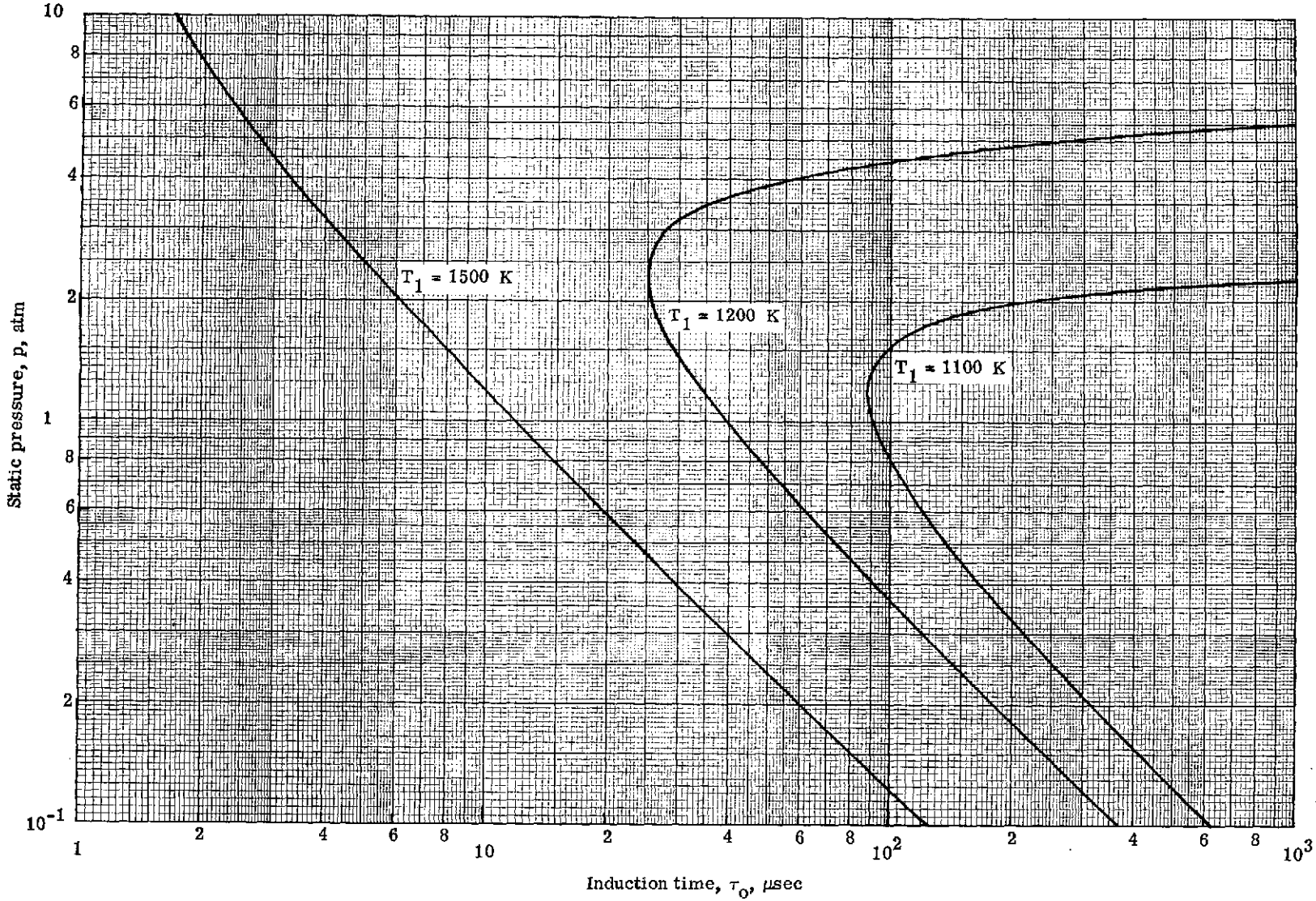

Figure 10.- Induction-time variation with static pressure for a family of initial temperatures for $\phi = 1.0$ and $X_O = 0$.

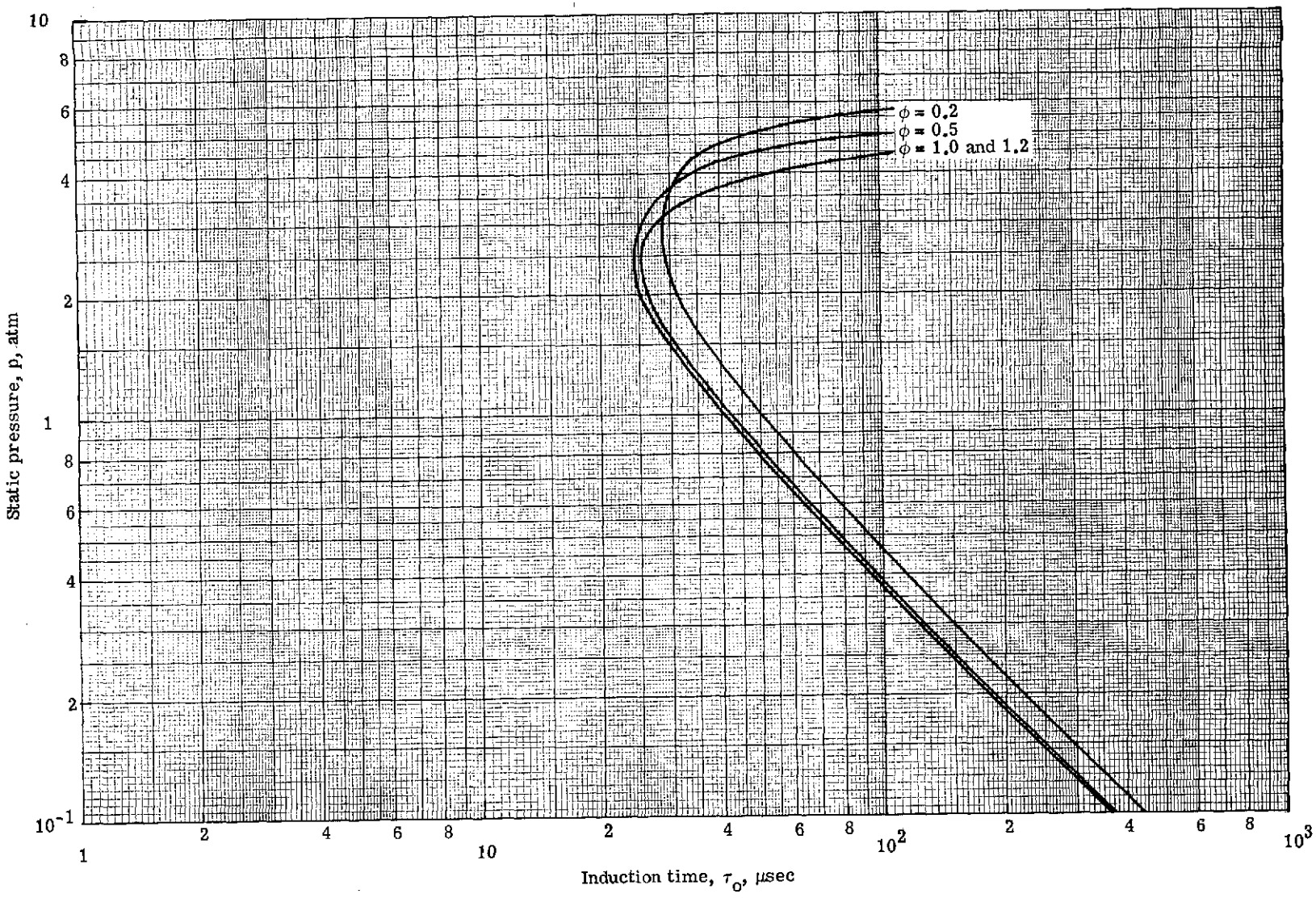

Figure 11.- Induction-time variation with static pressure for a family of equivalence ratios for T_1 = 1200 K and X_O = 0.

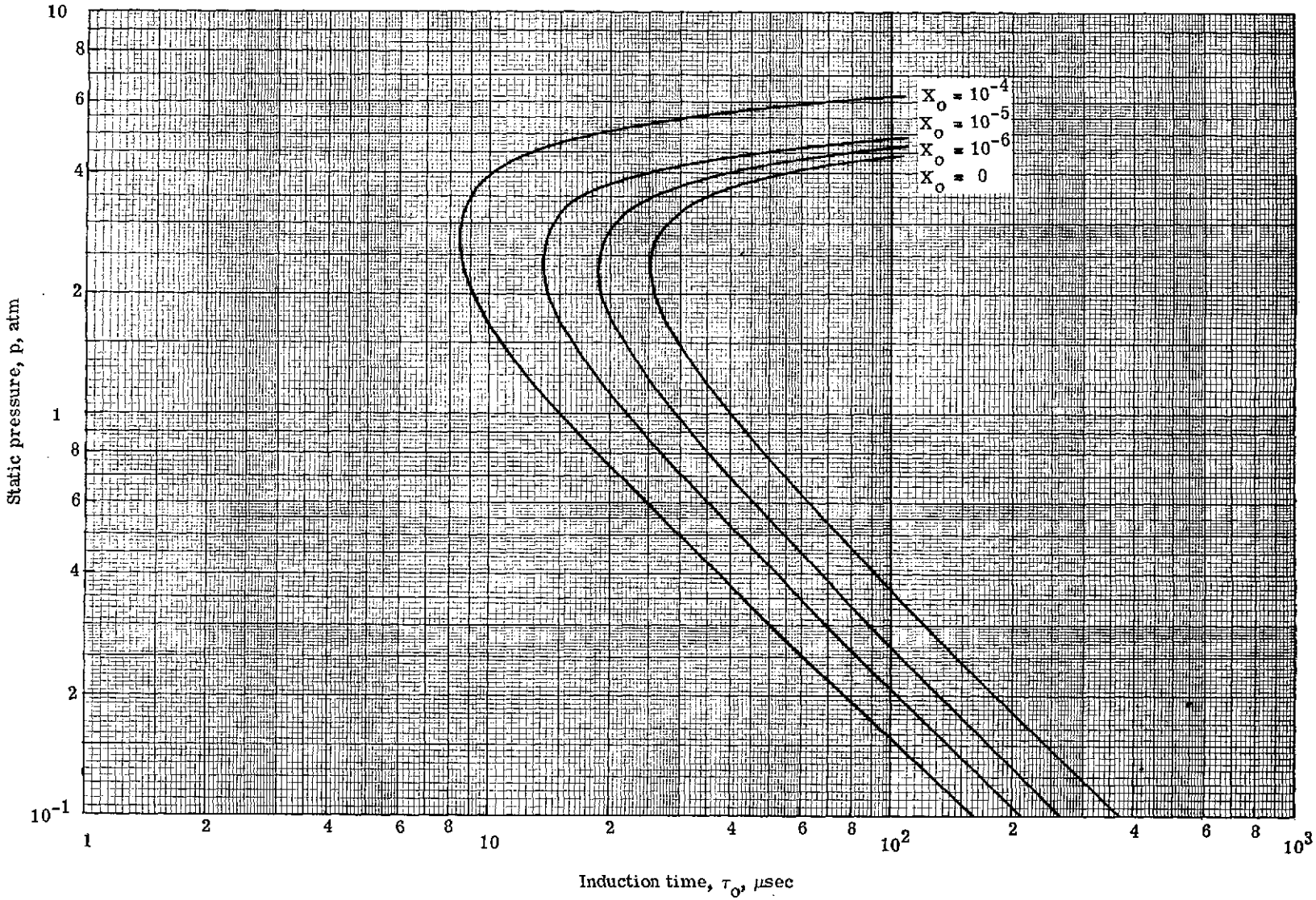

Figure 12.- Induction-time variation with static pressure for a family of initial mole fractions of atomic oxygen for $T_1 = 1200$ K and $\phi = 1.0$.

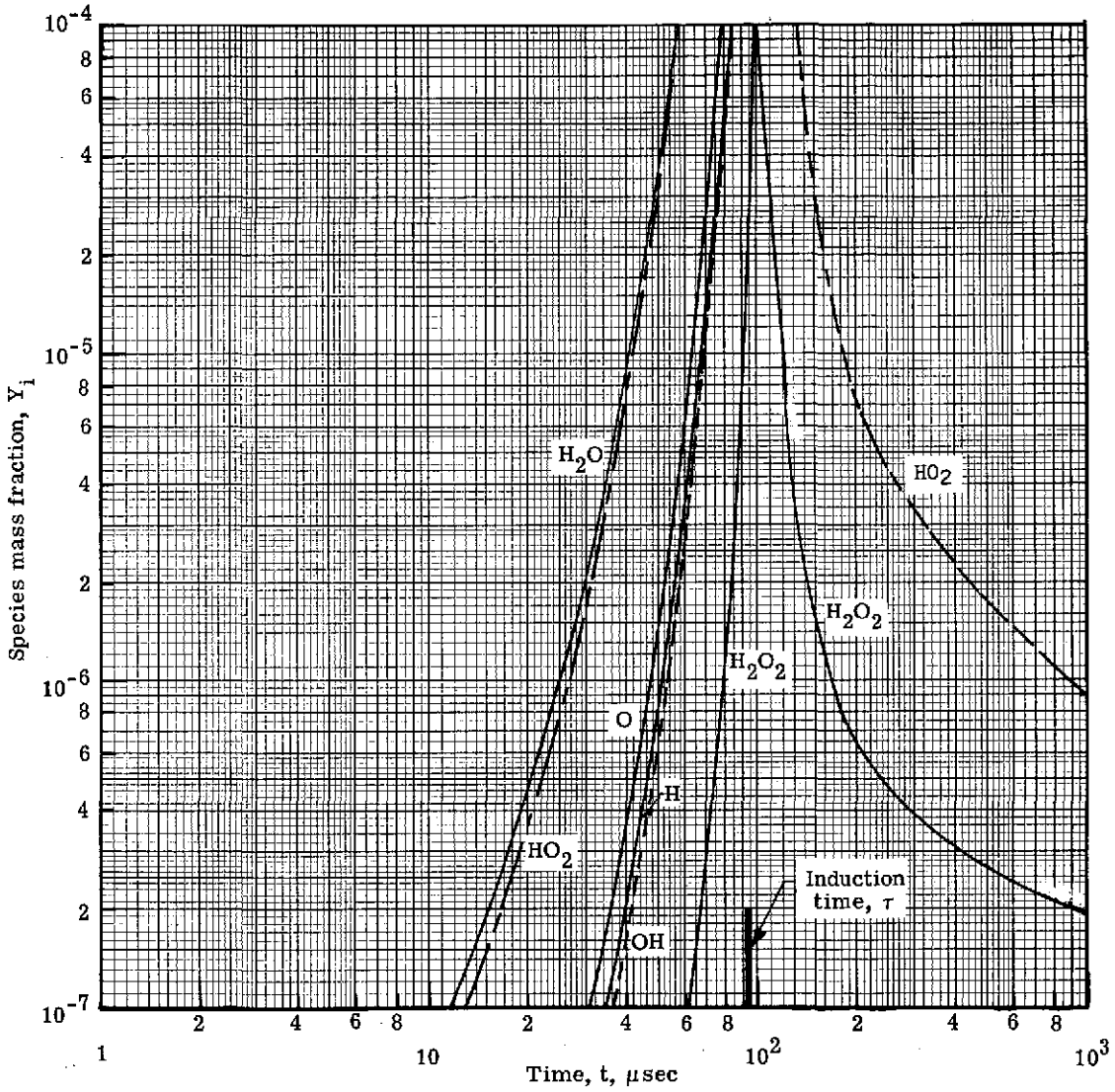

(a) Mass fraction, 10^{-7} to 10^{-4}.

Figure 13.- Time variation of species mass fraction for T_1 = 1100 K, p = 1.0 atm, ϕ = 1.0, and X_O = 0.

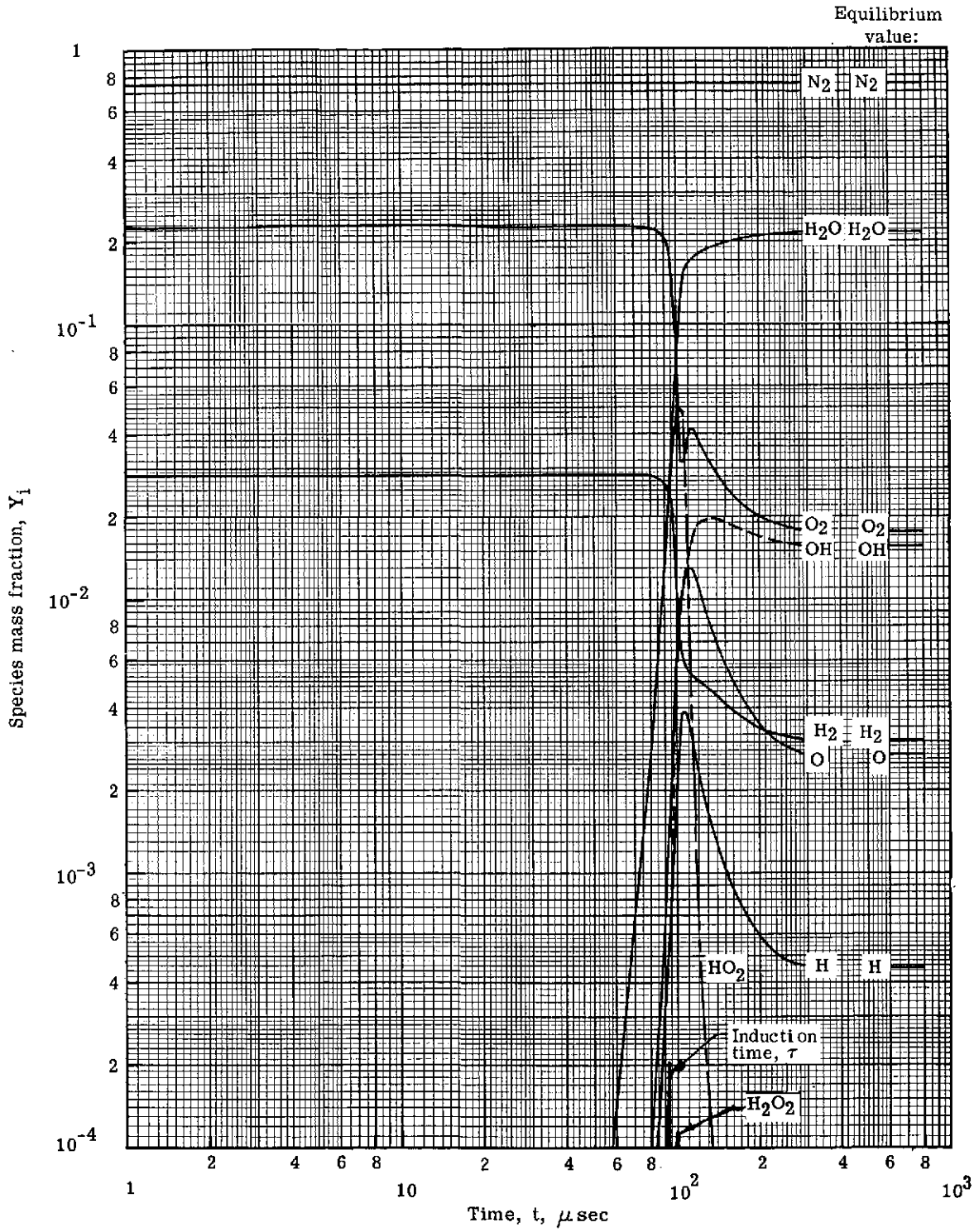

(b) Mass fraction, 10^{-4} to 1.

Figure 13.- Concluded.

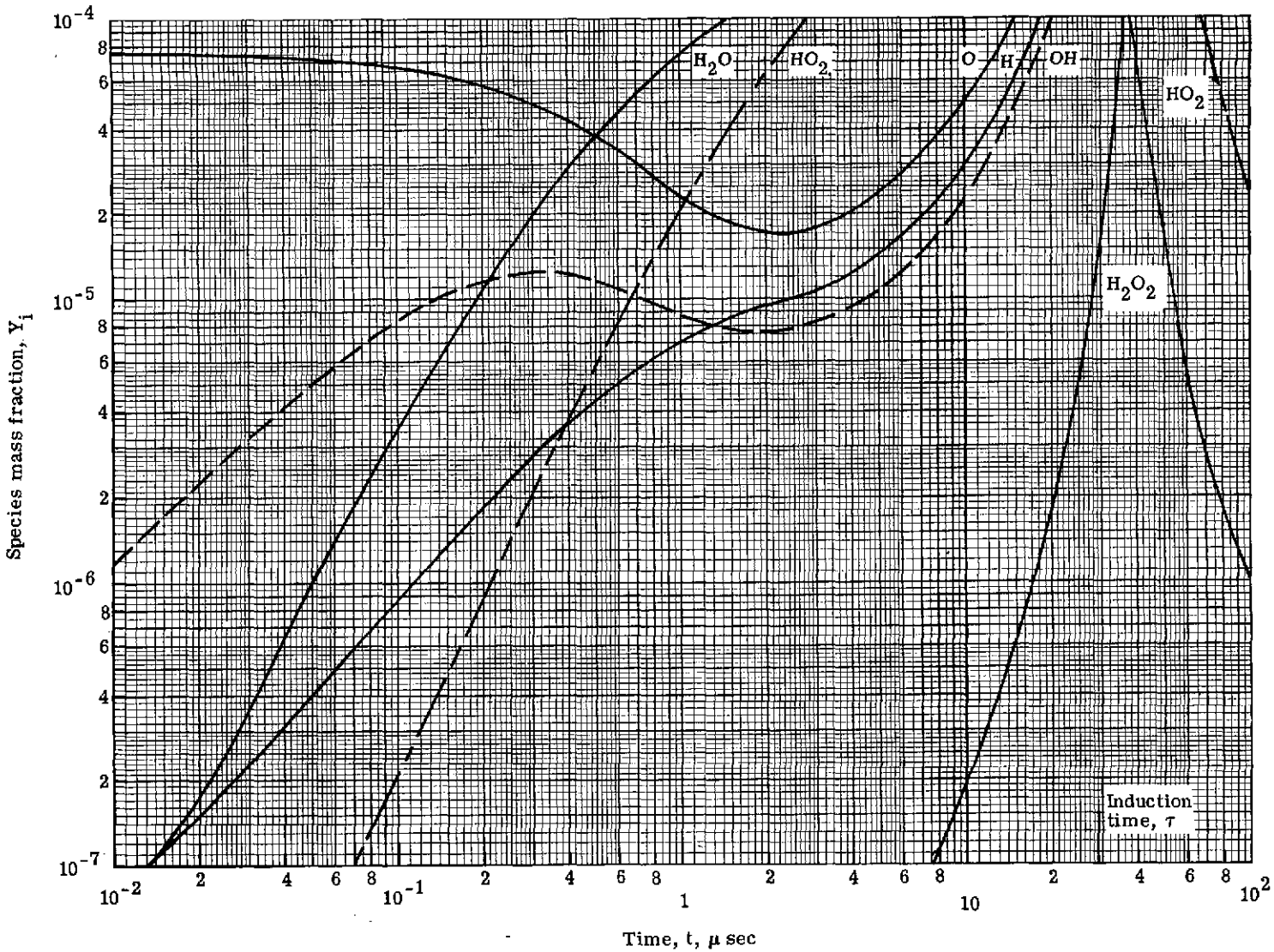

(a) Mass fraction, 10^{-7} to 10^{-4}.

Figure 14.- Time variation of species mass fraction for $T_1 = 1100$ K, $p = 1.0$ atm, $\phi = 1.0$, and $X_O = 10^{-4}$.

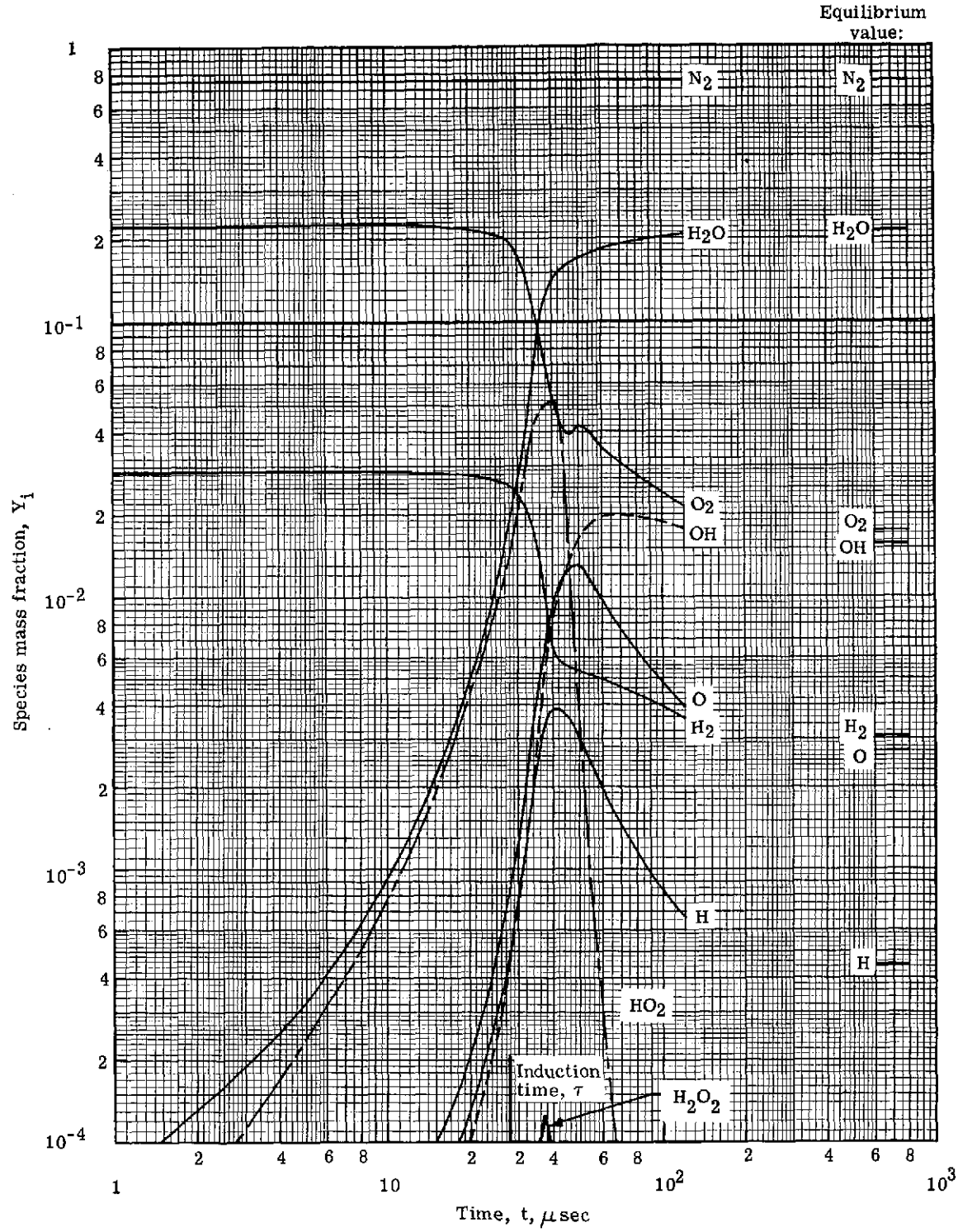

(b) Mass fraction, 10^{-4} to 1.

Figure 14.- Concluded.

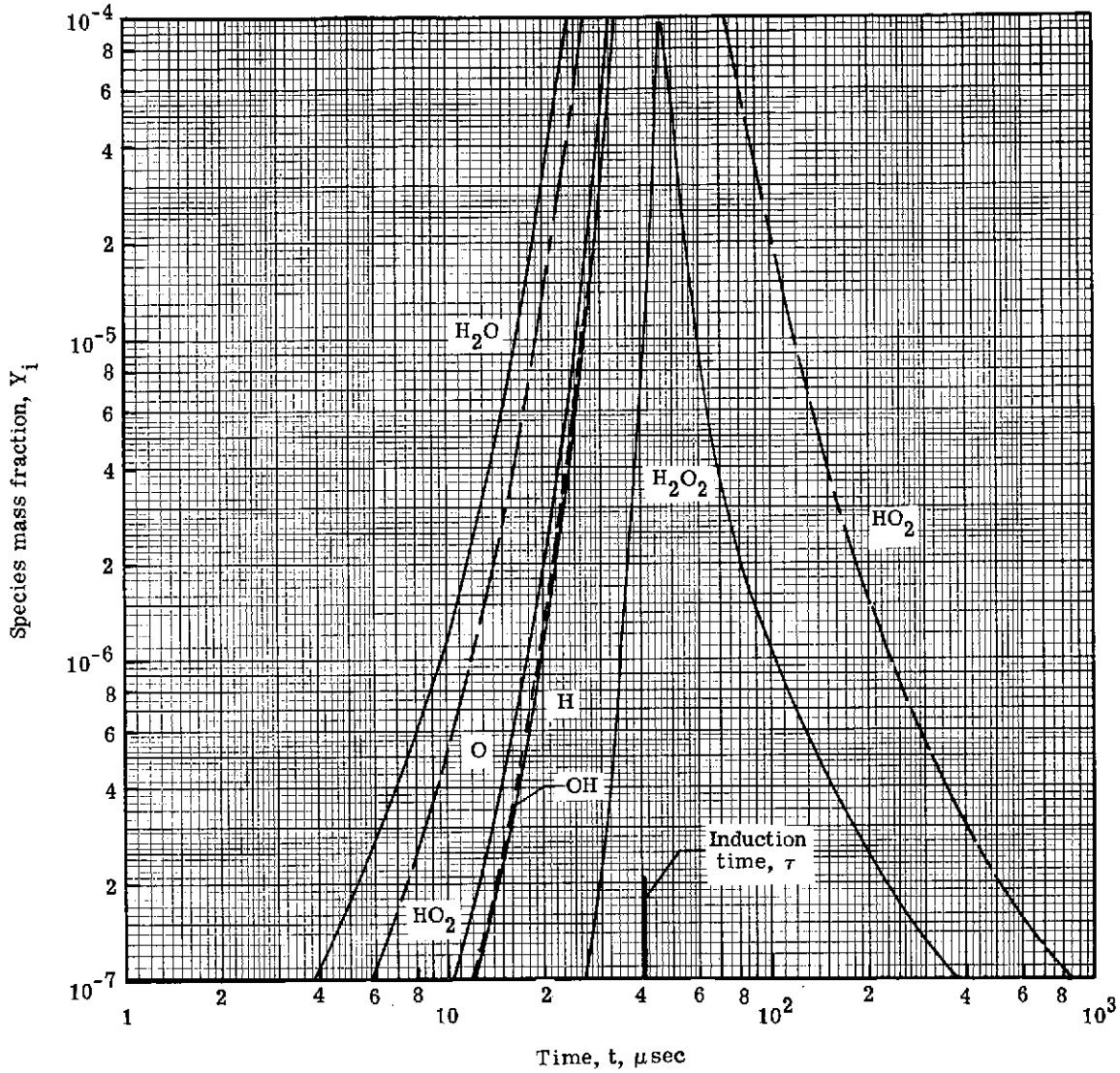

(a) Mass fraction, 10^{-7} to 10^{-4}.

Figure 15.- Time variation of species mass fraction for T_1 = 1200 K, p = 1.0 atm, ϕ = 1.0, and X_O = 0.

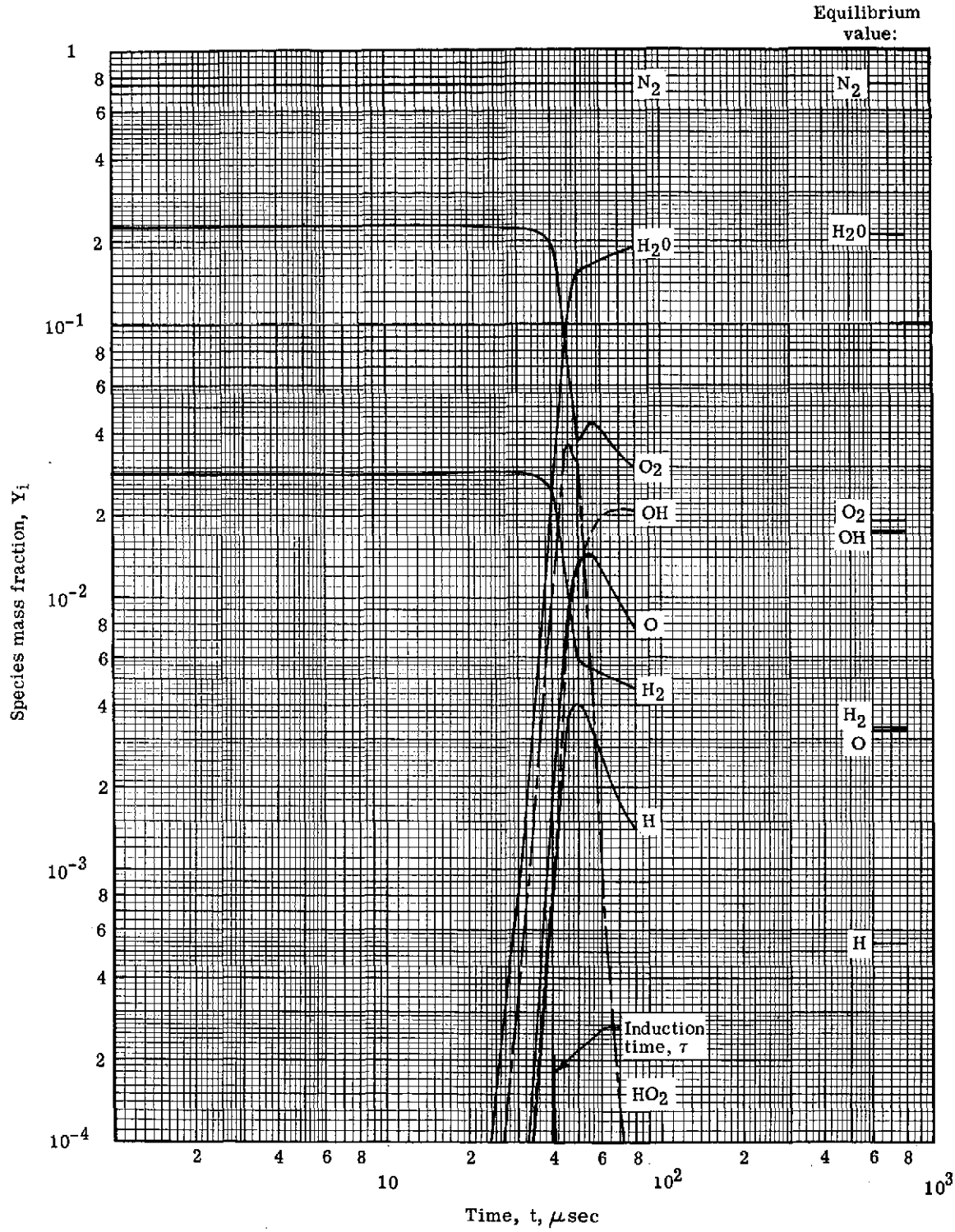

(b) Mass fraction, 10^{-4} to 1.

Figure 15.- Concluded.

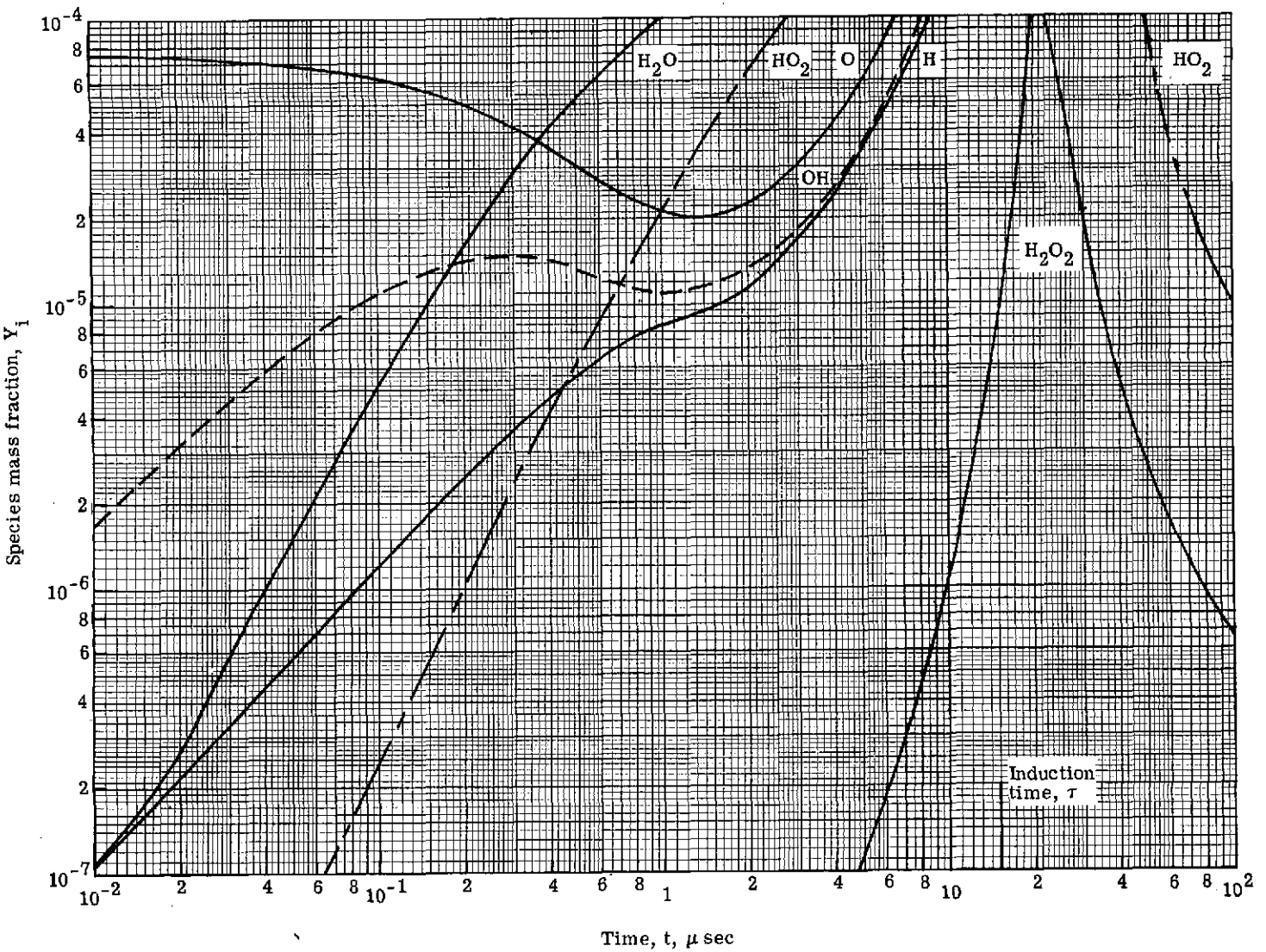

(a) Mass fraction, 10^{-7} to 10^{-4}.

Figure 16.- Time variation of species mass fraction for T_1 = 1200 K, p = 1.0 atm, ϕ = 1.0, and $X_O = 10^{-4}$.

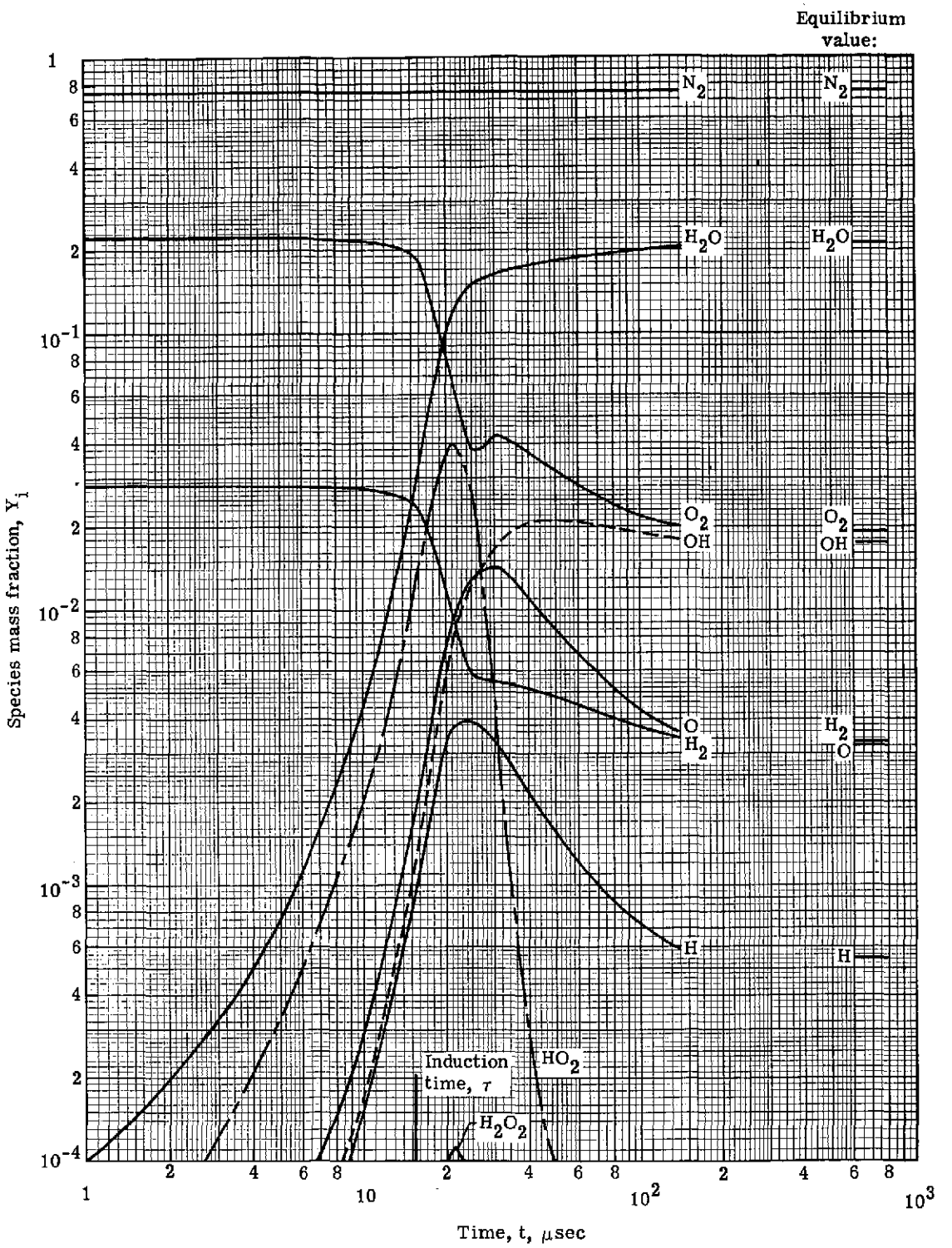

(b) Mass fraction, 10^{-4} to 1.

Figure 16.- Concluded.

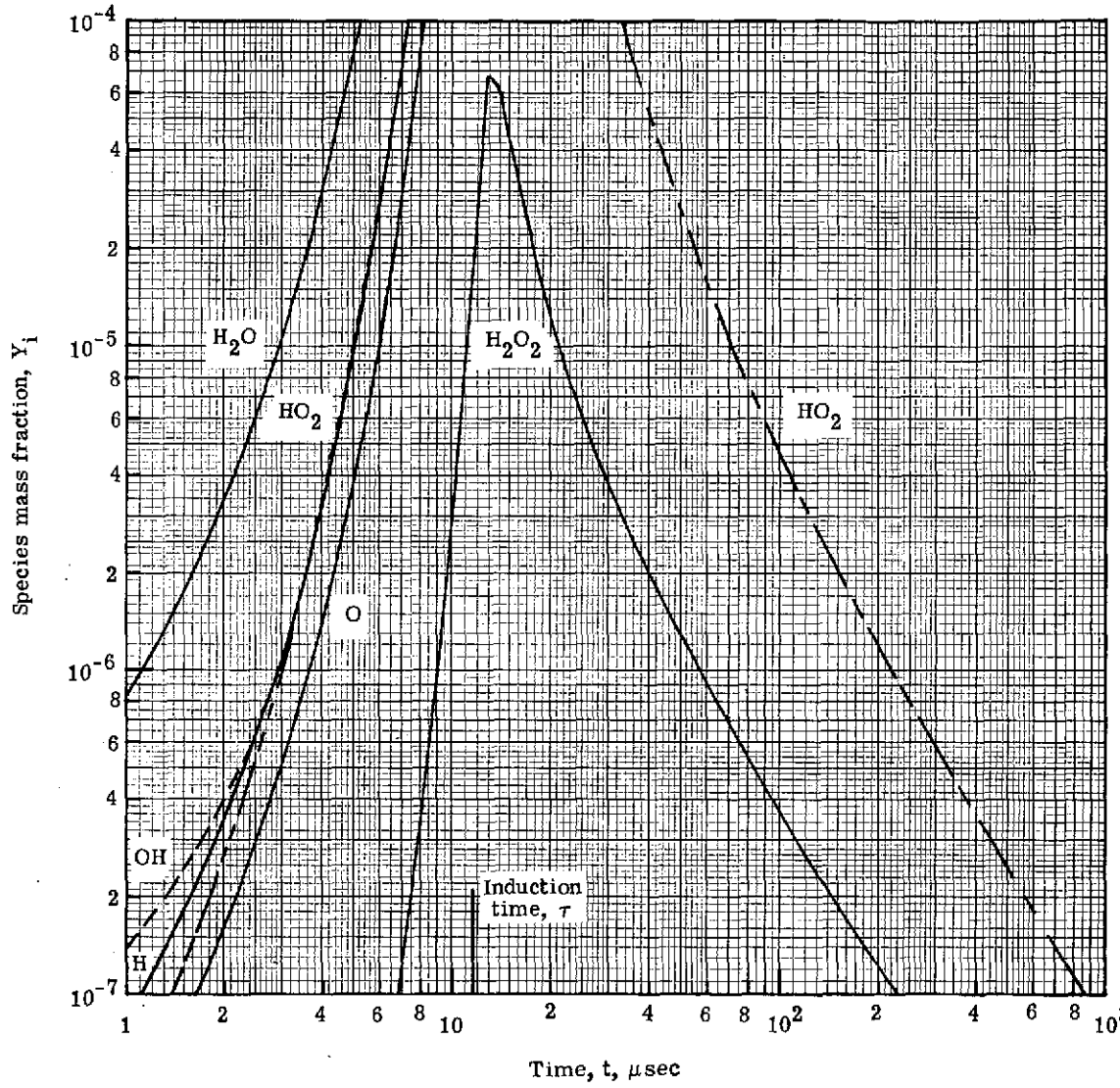

(a) Mass fraction, 10^{-7} to 10^{-4}.

Figure 17.- Time variation of species mass fraction for T_1 = 1500 K, p = 1.0 atm, ϕ = 1.0, and X_O = 0.

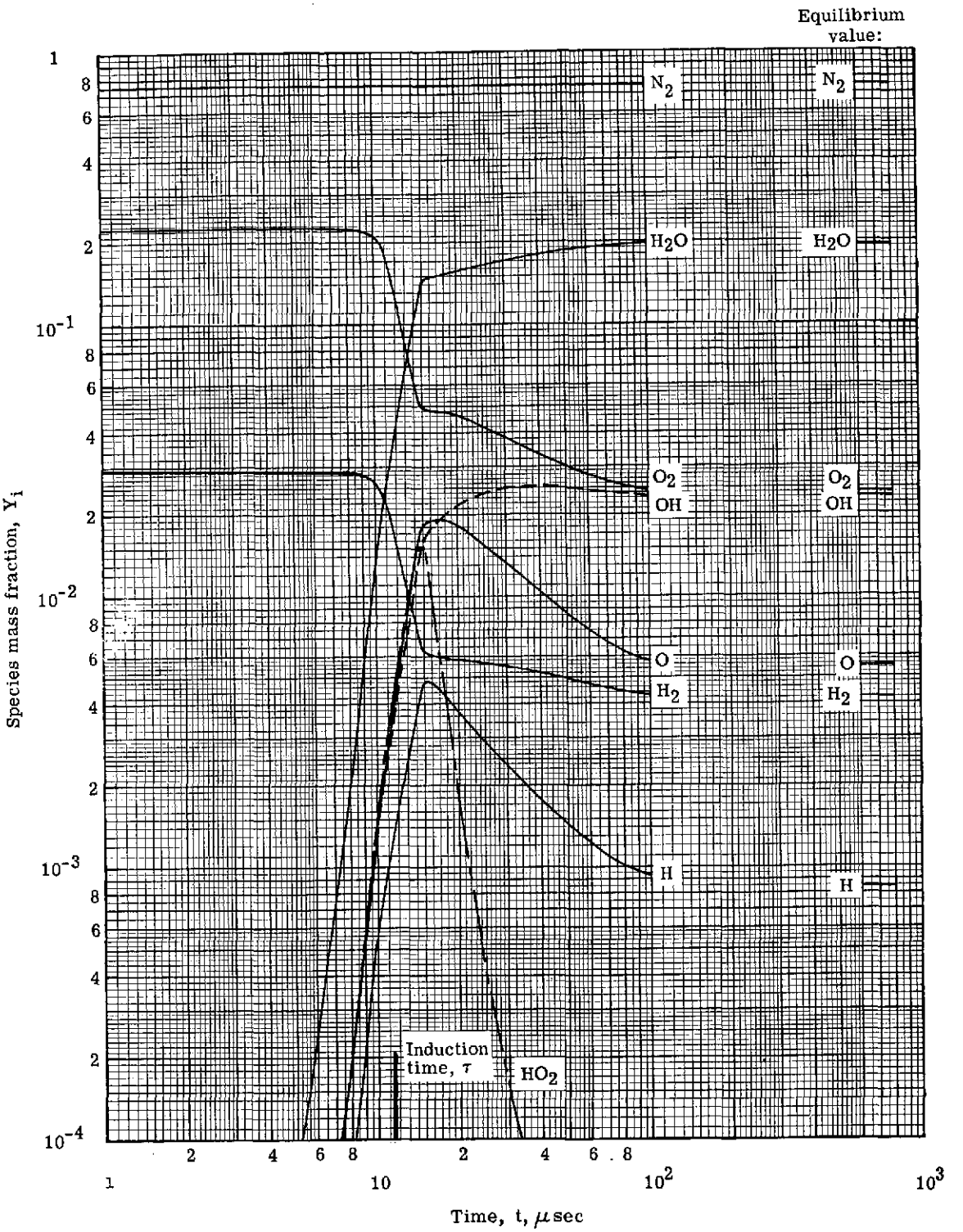

(b) Mass fraction, 10^{-4} to 1.

Figure 17.- Concluded.

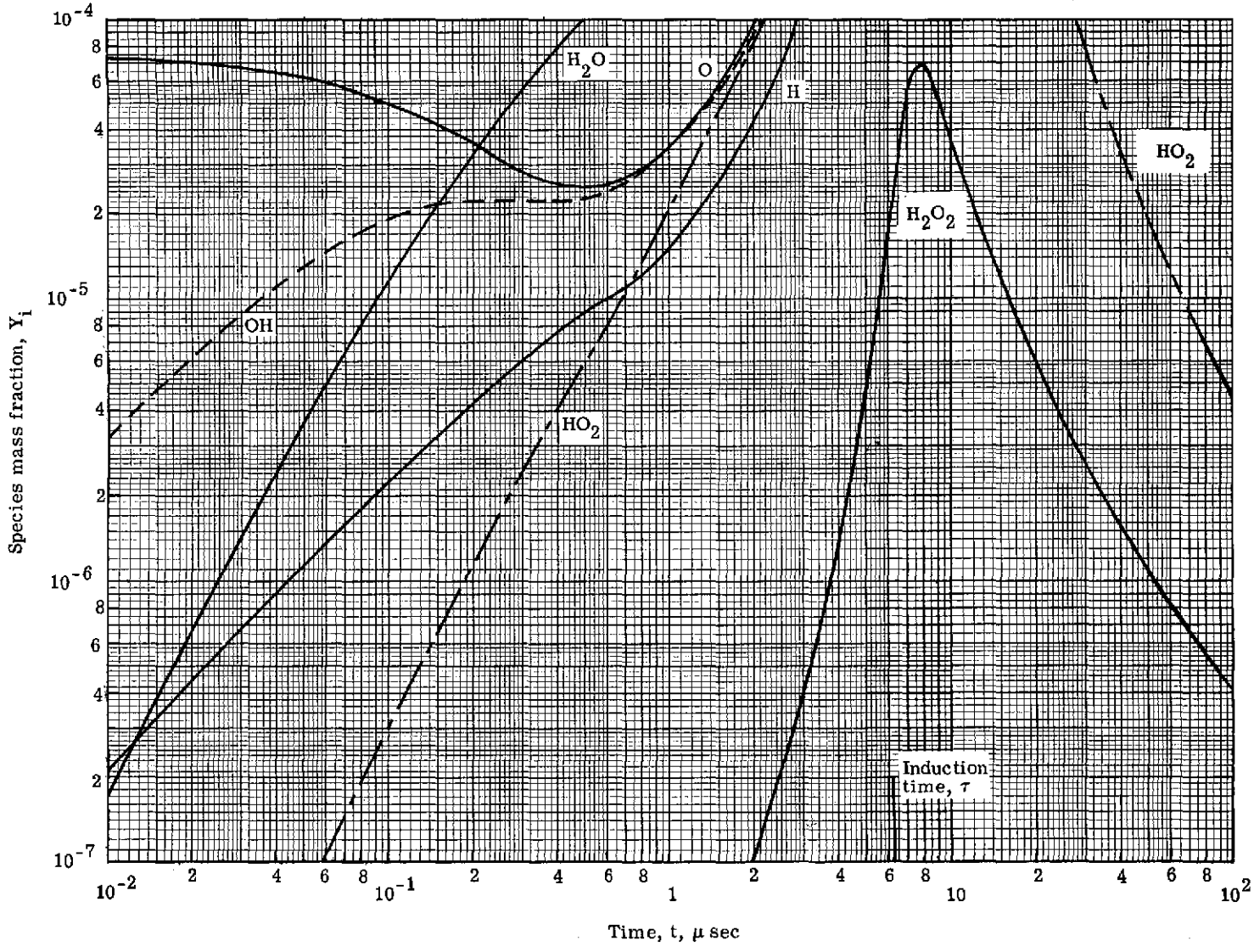

(a) Mass fraction, 10^{-7} to 10^{-4}.

Figure 18.- Time variation of species mass fraction for $T_1 = 1500$ K, $p = 1.0$ atm, $\phi = 1.0$, and $X_O = 10^{-4}$.

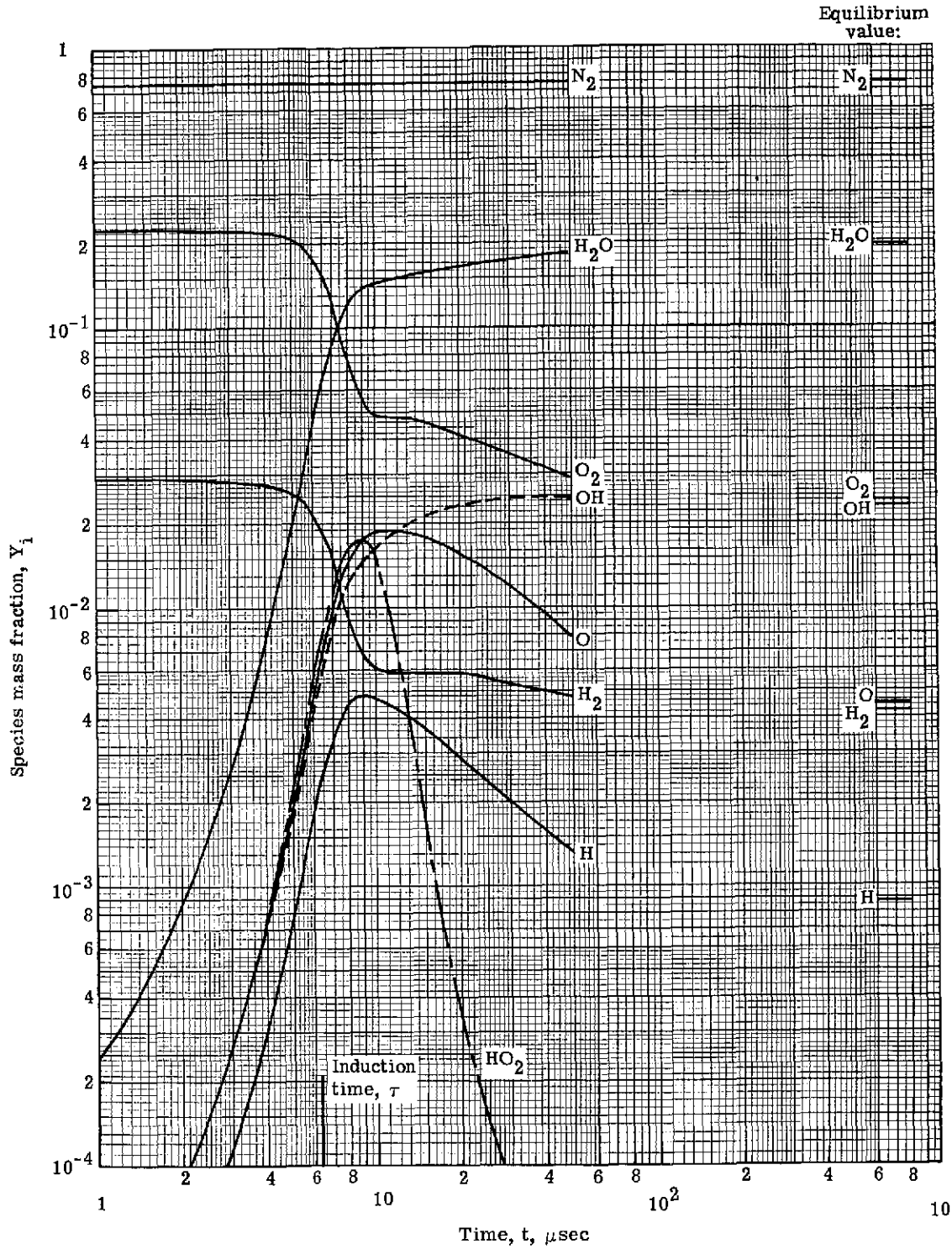

(b) Mass fraction, 10^{-4} to 1.

Figure 18.- Concluded.

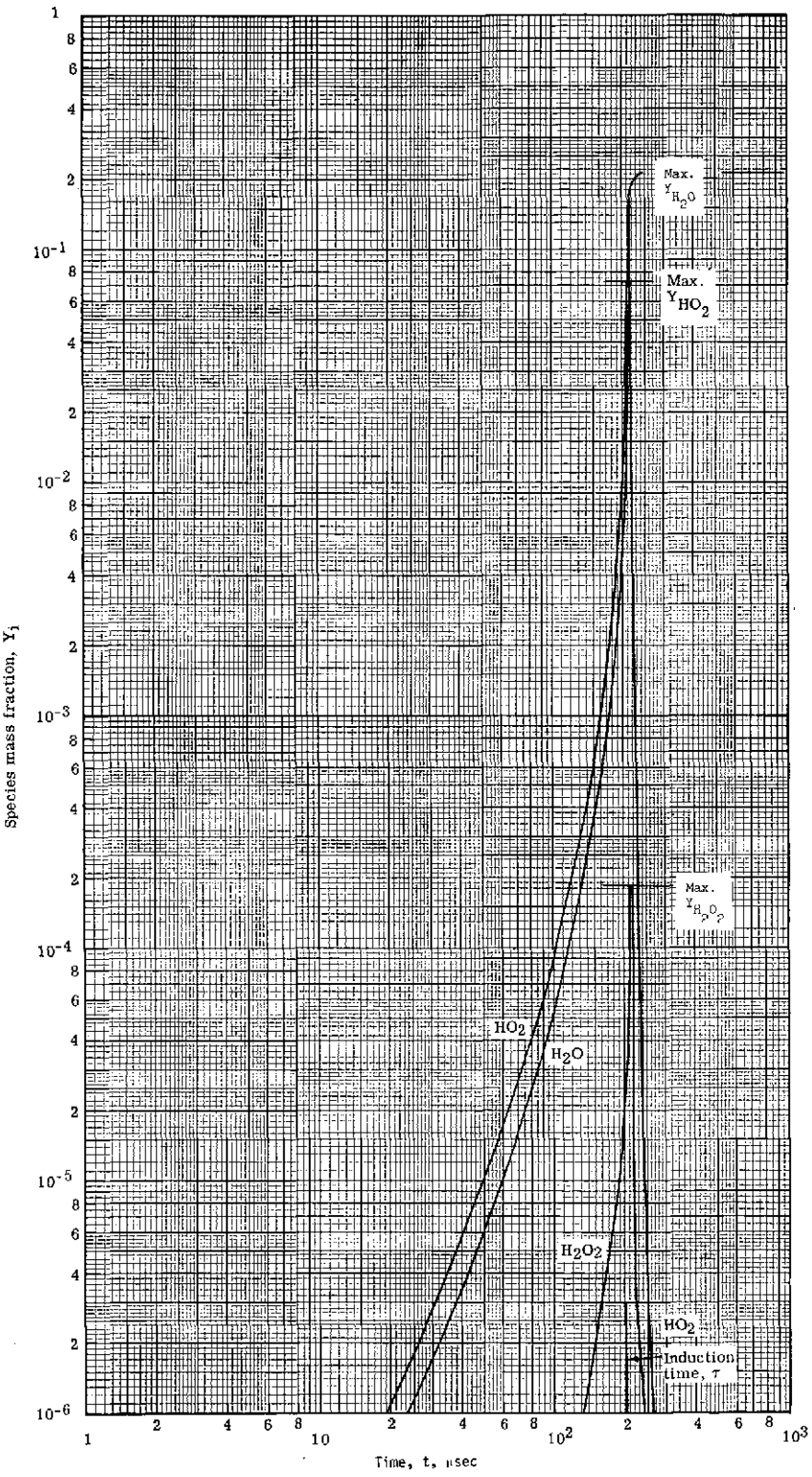

Figure 19.- Time variation of the mass fraction of H_2O, HO_2, H_2O_2 for T_1 = 1100 K, p = 2.0 atm, and ϕ = 1.0.

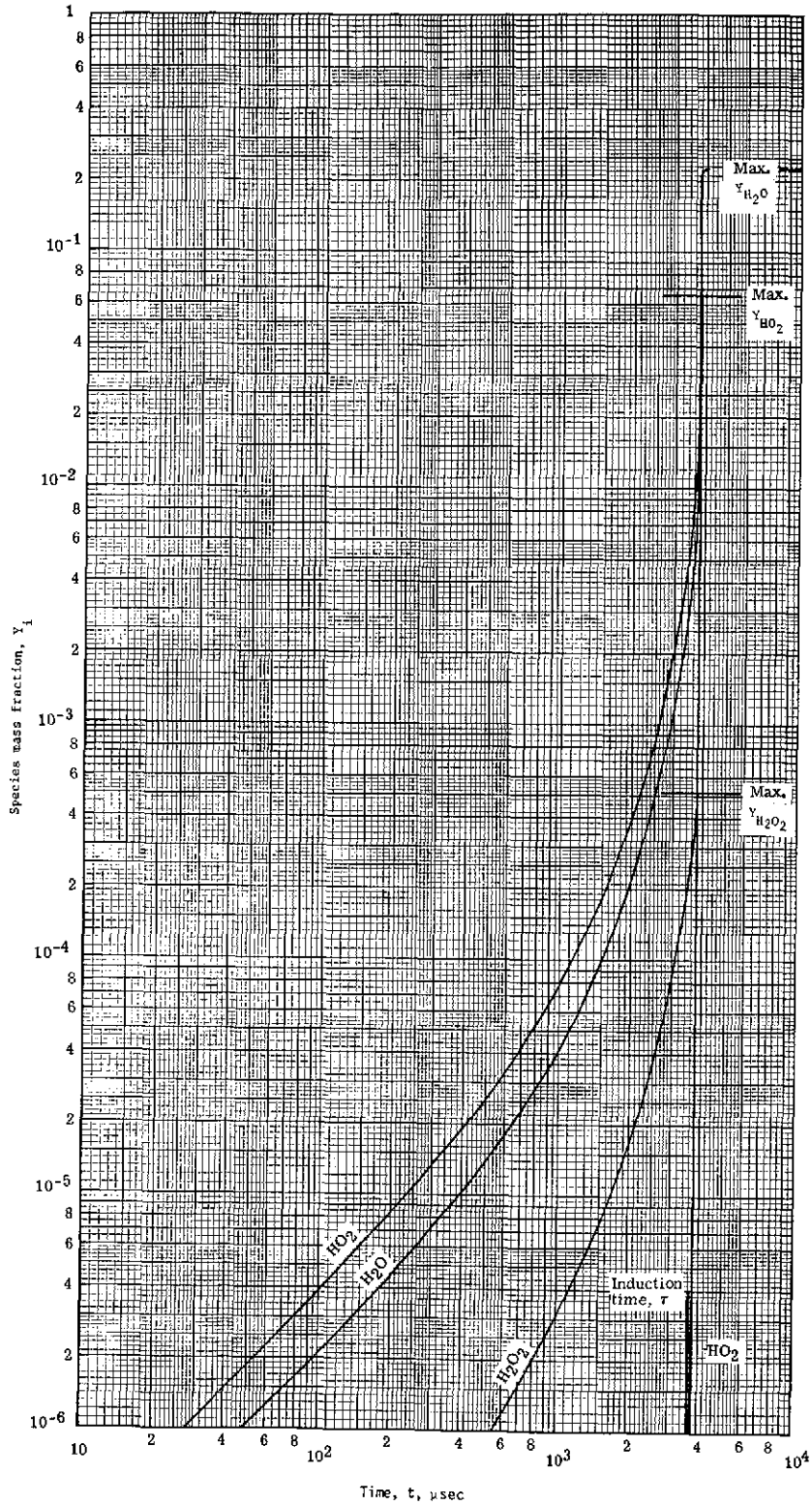

Figure 20.- Time variation of the mass fraction of H_2O, HO_2, and H_2O for T_1 = 1100 K, p = 4.0 atm, and ϕ = 1.0.

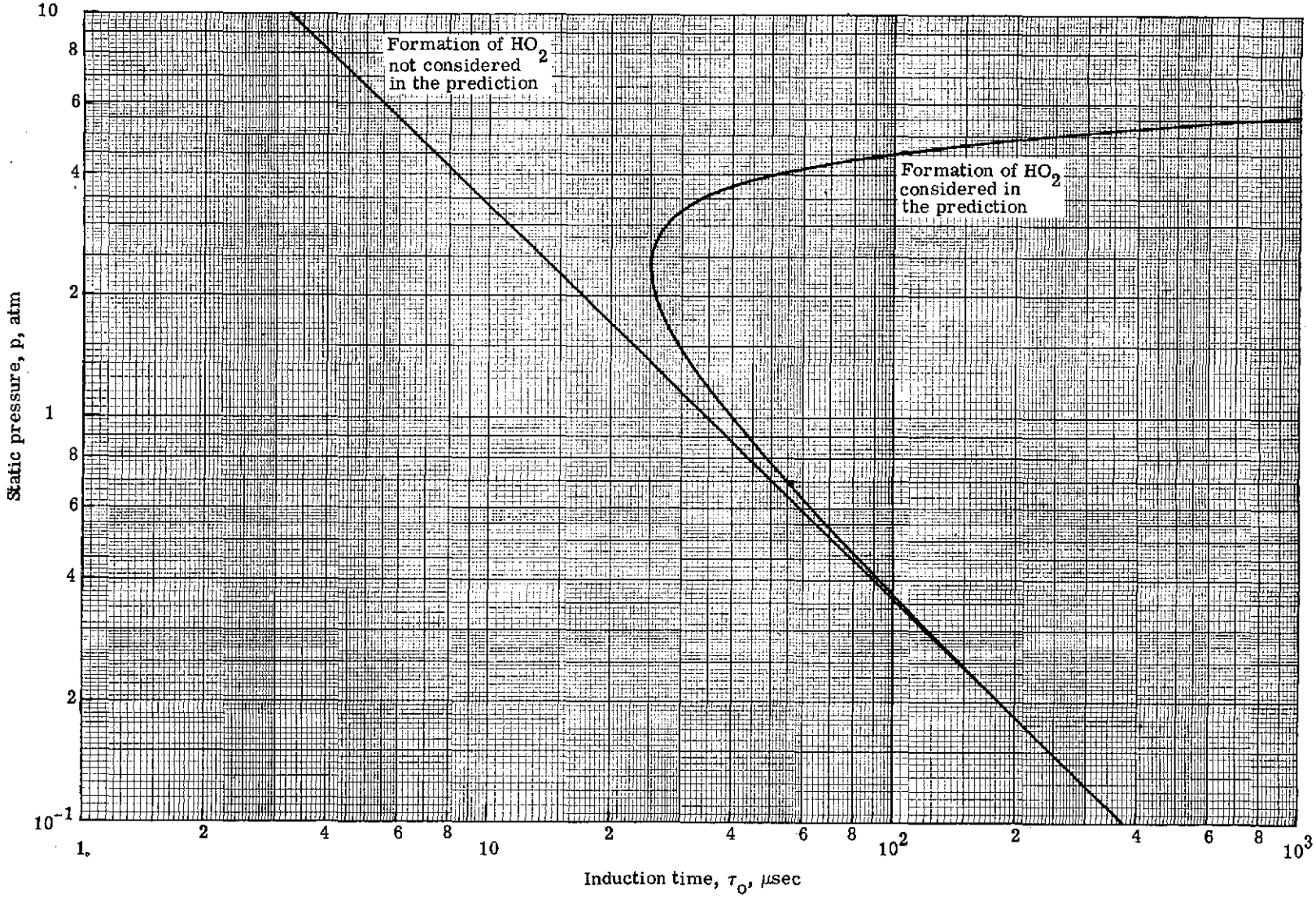

Figure 21.- Induction time variation with static pressure, considering and not considering hydroperoxyl for $T_1 = 1200$ K and $\phi = 1.0$.

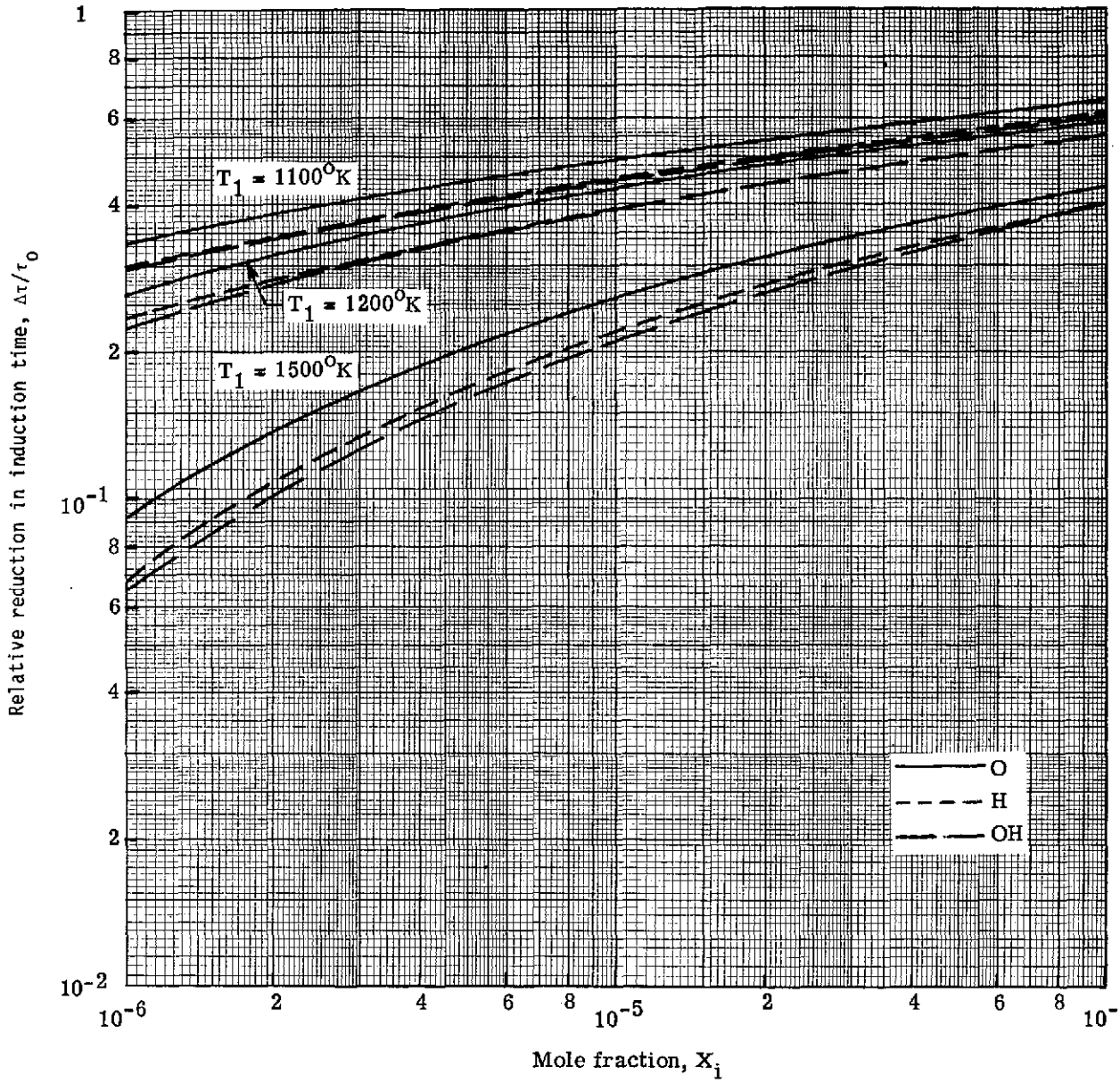

Figure 22.- Relative reduction in induction time as a function of mole fraction of atomic oxygen, atomic hydrogen, and hydroxyl for $p = 0.5$ atm and $\phi = 1.0$.

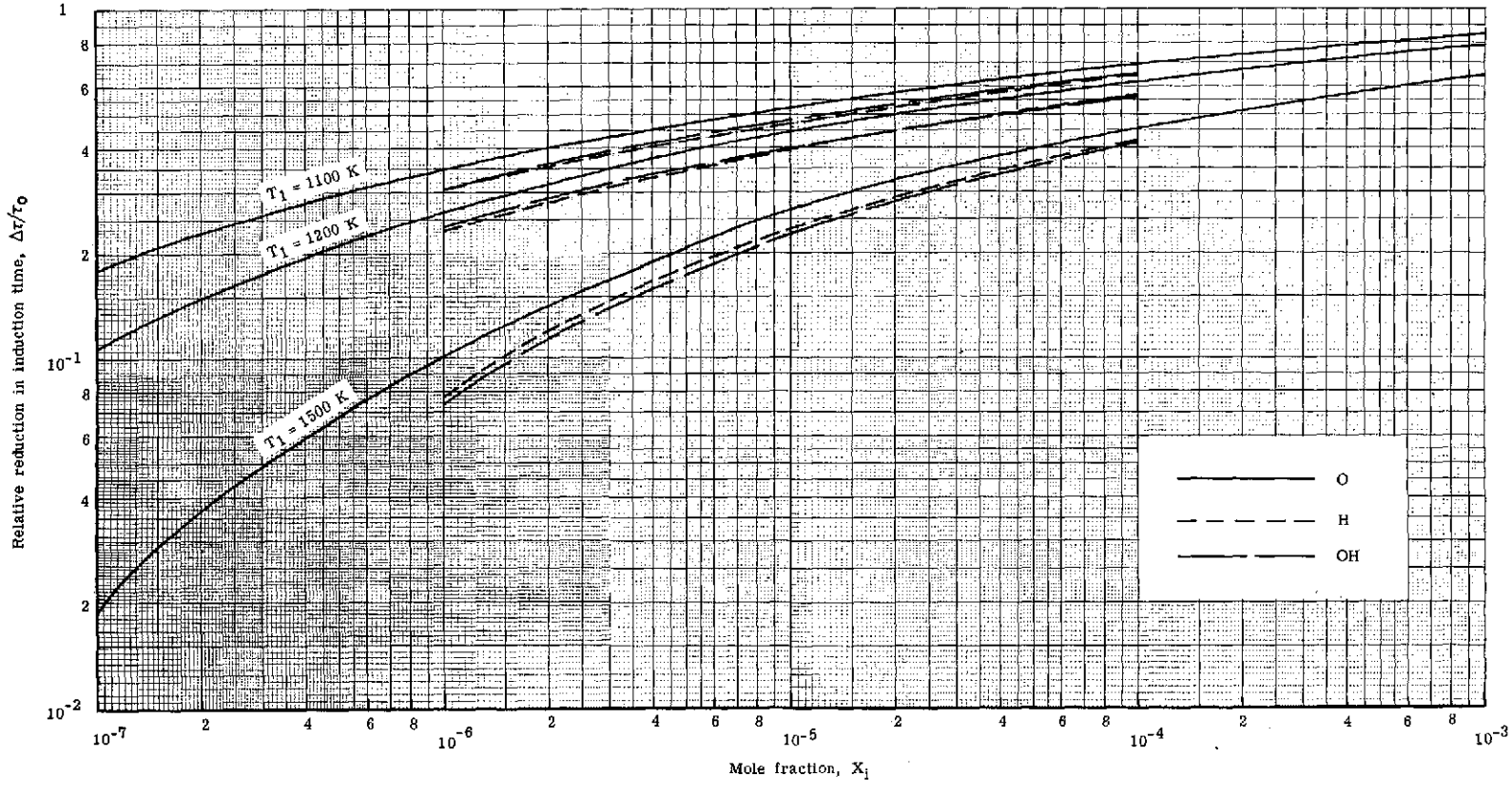

Figure 23.- Relative reduction in induction time as a function of mole fraction of atomic oxygen, atomic hydrogen, and hydroxyl for $p = 1.0$ atm and $\phi = 1.0$.

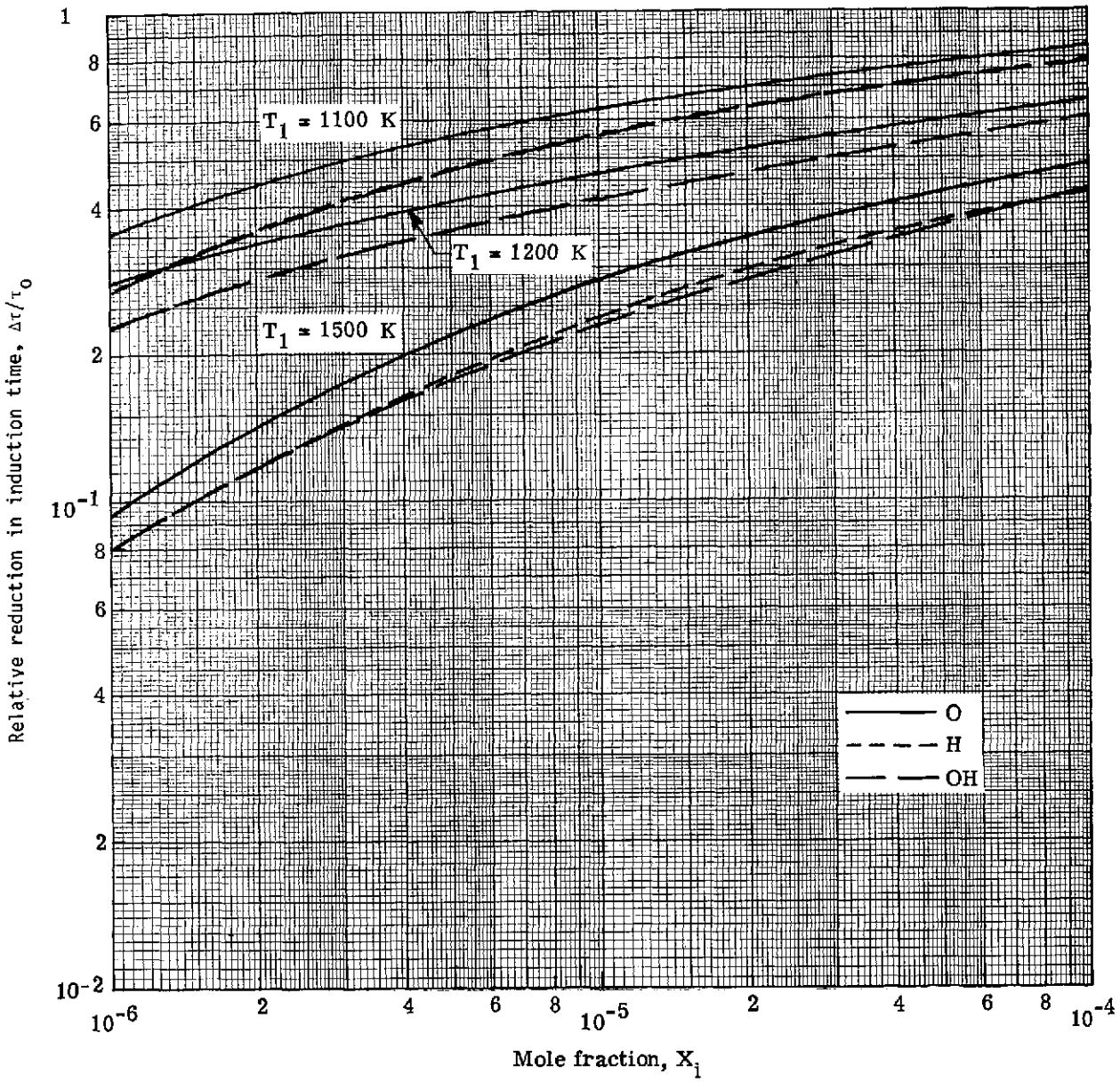

Figure 24. - Relative reduction in induction time as a function of mole fraction of atomic oxygen, atomic hydrogen, and hydroxyl for $p = 2.0$ atm and $\phi = 1.0$.

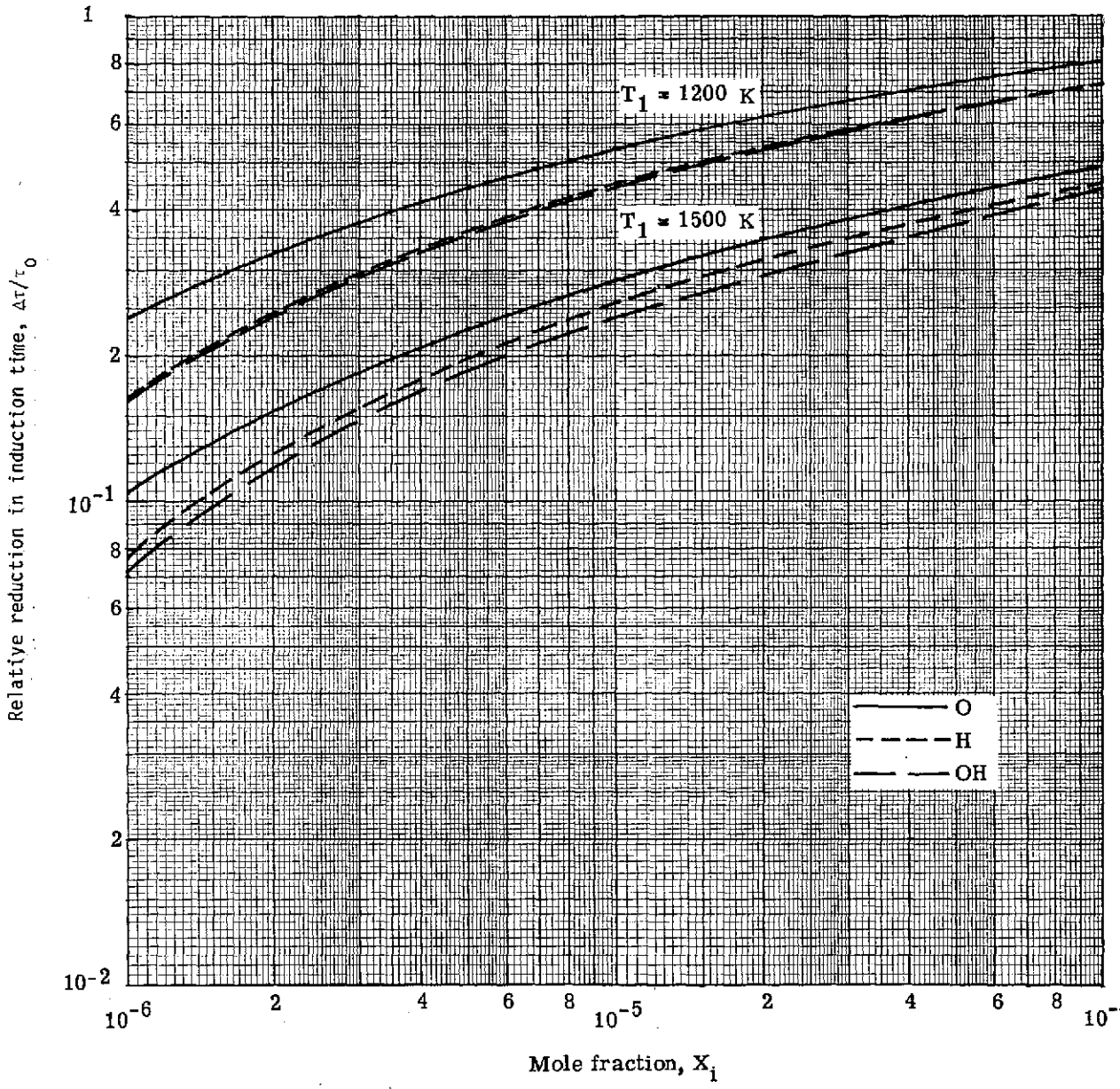

Figure 25.- Relative reduction in induction time as a function of mole fraction of atomic oxygen, atomic hydrogen, and hydroxyl for p = 4.0 atm and ϕ = 1.0.

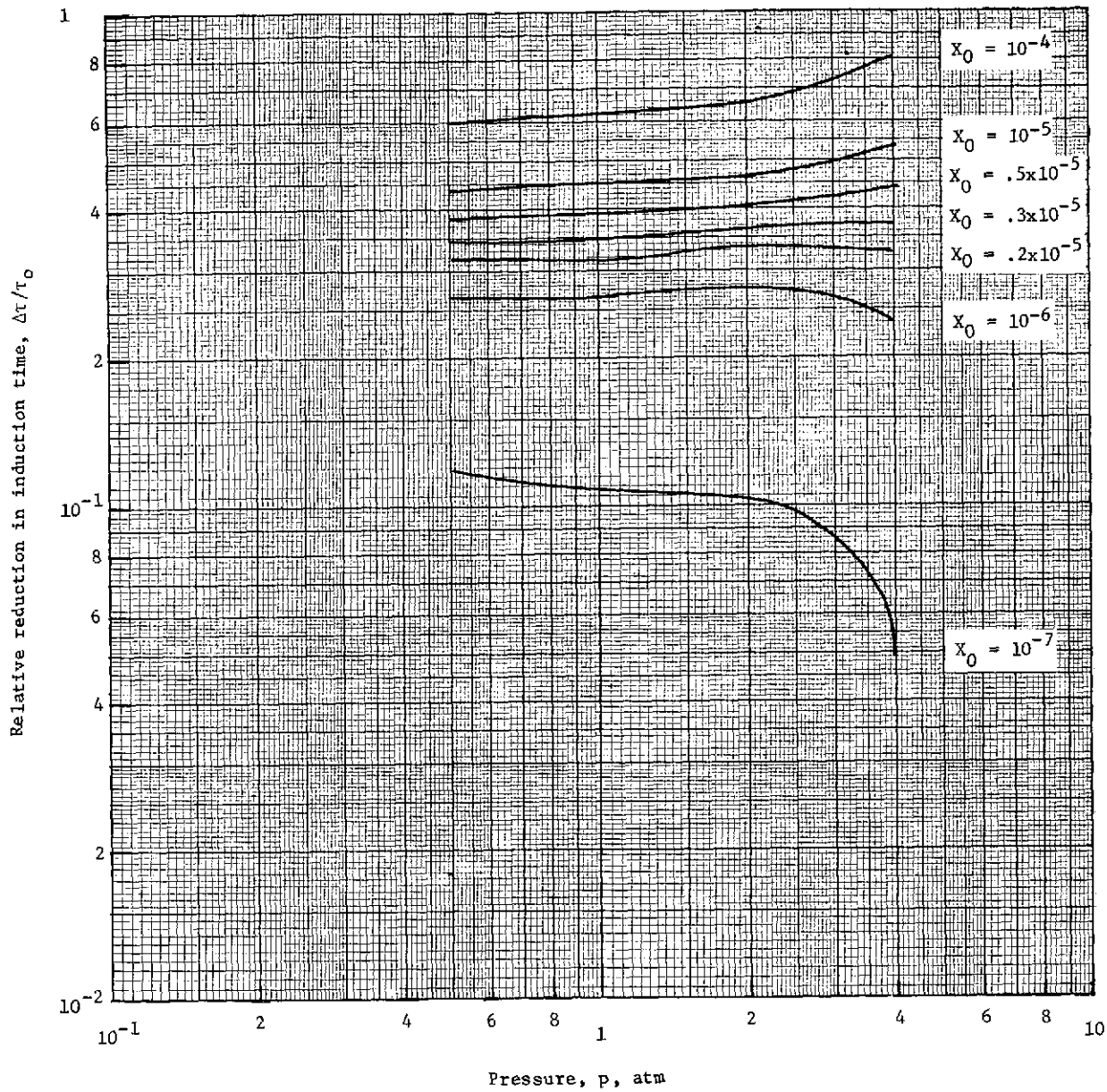

Figure 26.- Variation of relative reduction in induction time with pressure for $T_1 = 1200$ K and $\phi = 1.0$.

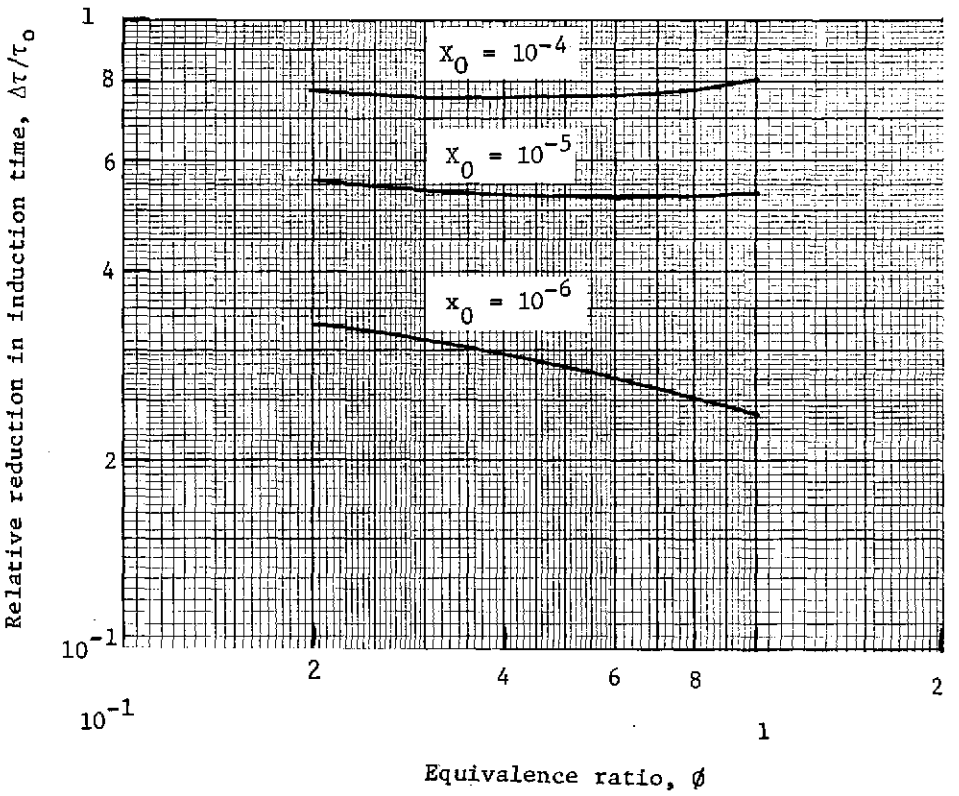

Figure 27.- Variation of relative reduction in induction time with equivalence ratio for $T_1 = 1200$ K and $p = 4.0$ atm.

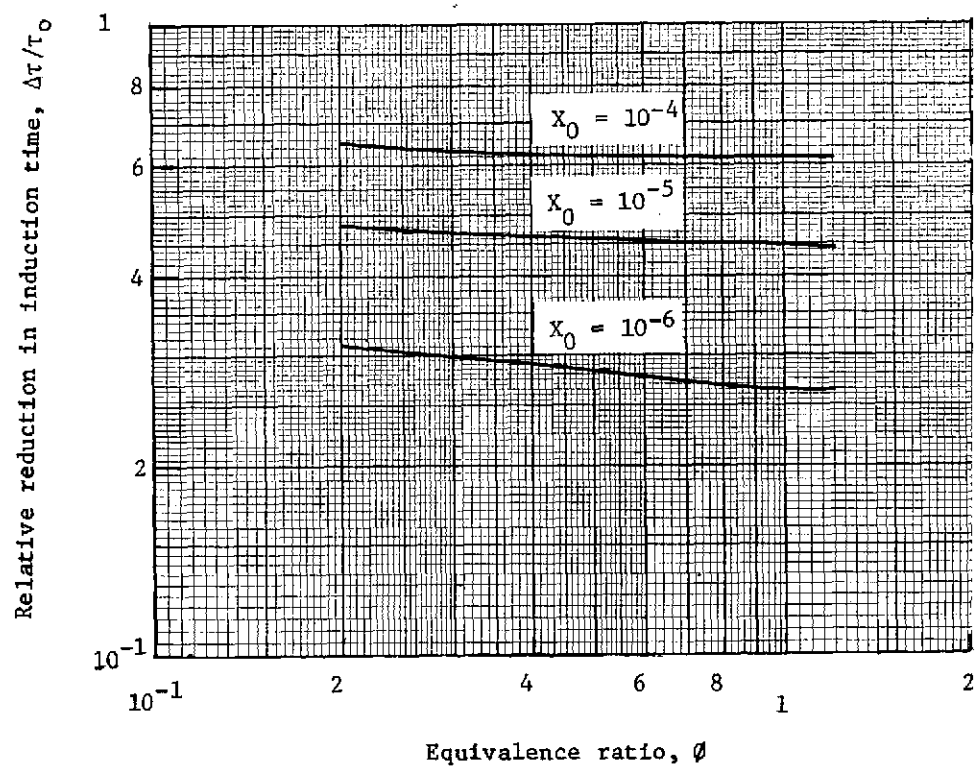

Figure 28.- Variation of relative reduction in induction time with equivalence ratio for $T_1 = 1200$ K and $p = 1.0$ atm.

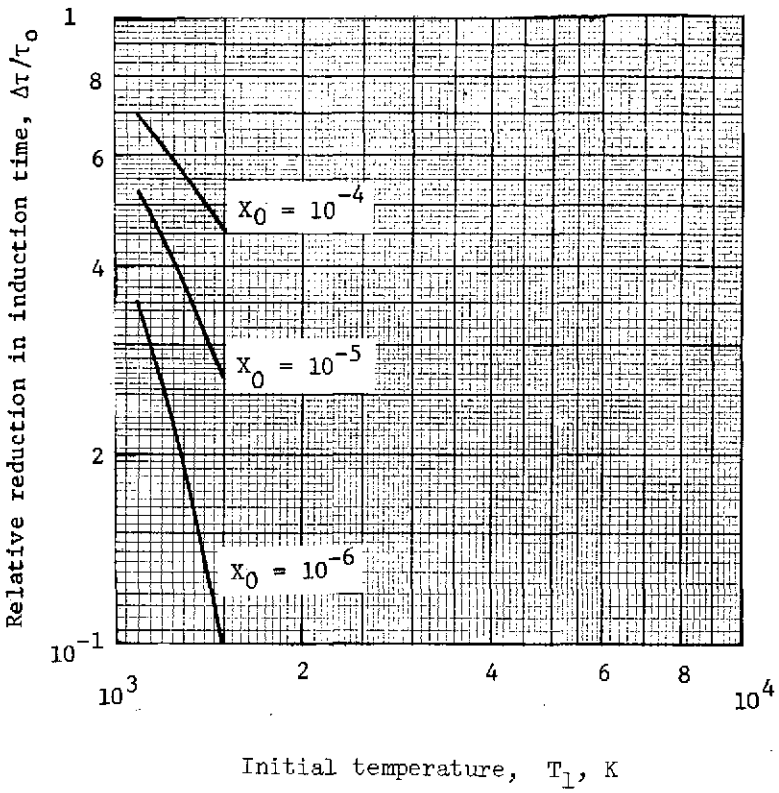

Figure 29.- Variation of relative reduction in induction time with initial temperature for $p = 1.0$ atm and $\phi = 1.0$.

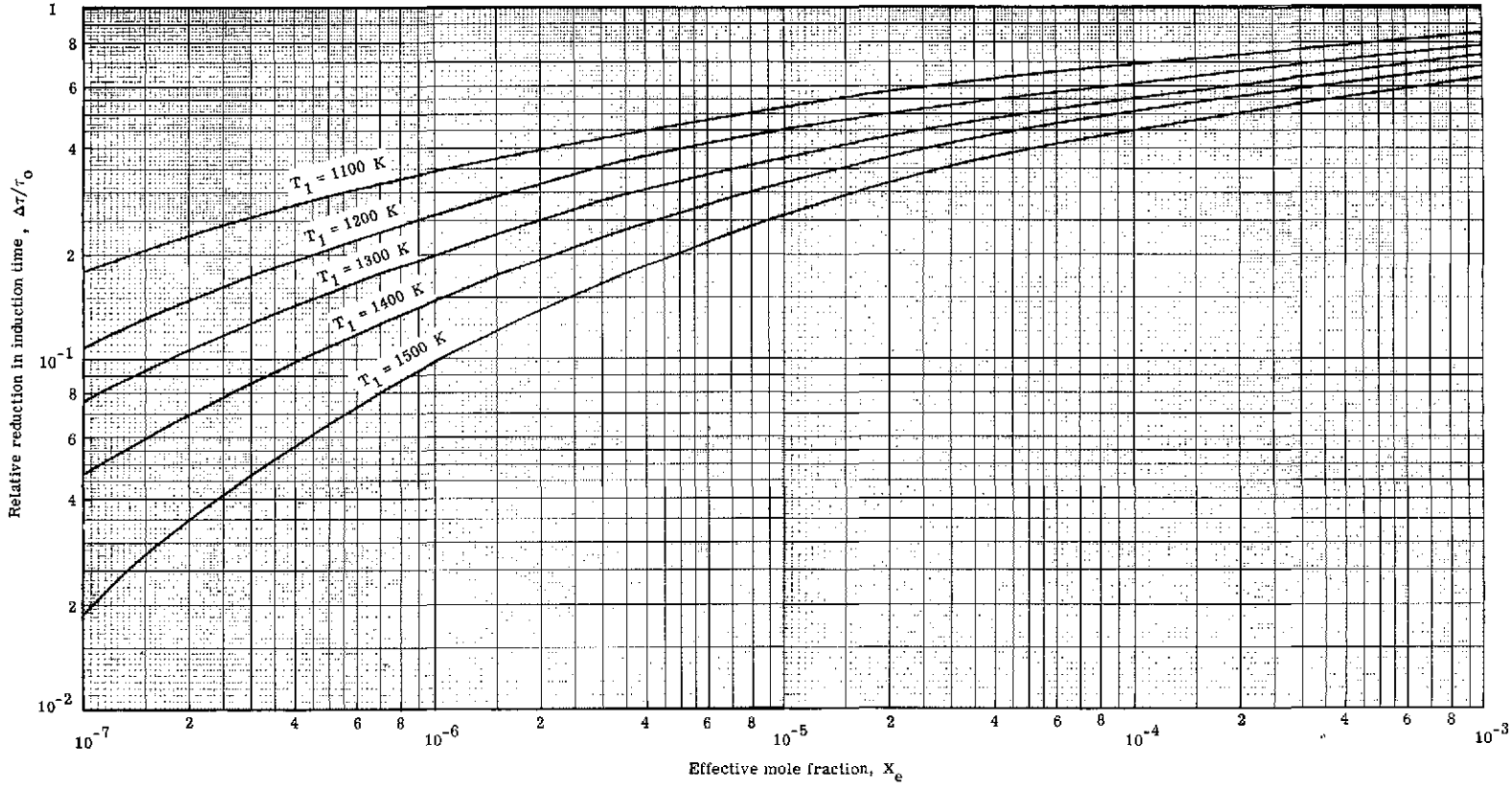

Figure 30.- Relative reduction in induction time as a function of effective mole fraction computed by empirical relationships for p = 1.0 atm and ϕ = 1.0.

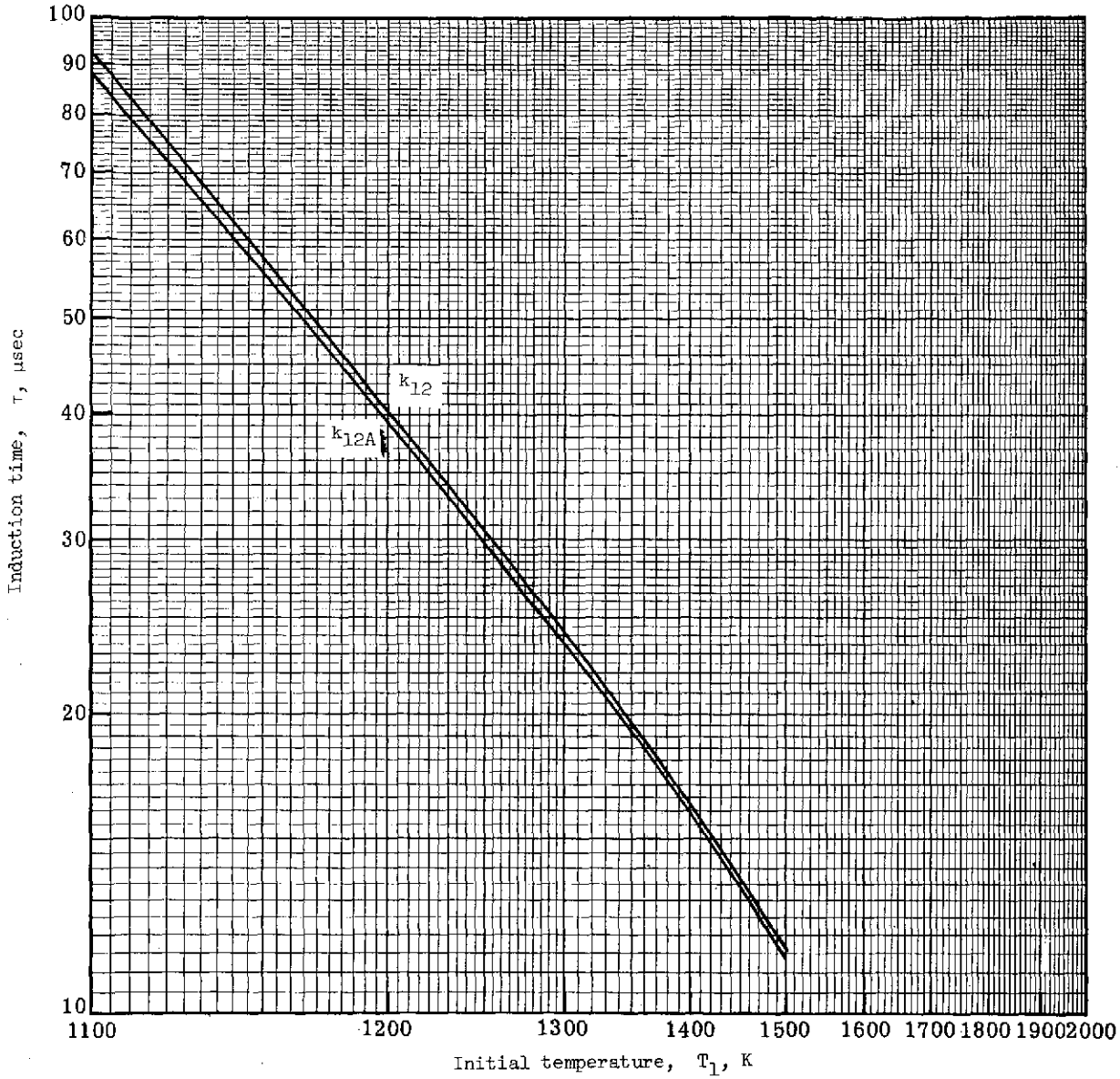

Figure 31.- Comparison of induction time for p = 1.0 atm and ϕ = 1.0 using the k_{12} and k_{12A} and X_O = 0 and 10^{-4}.

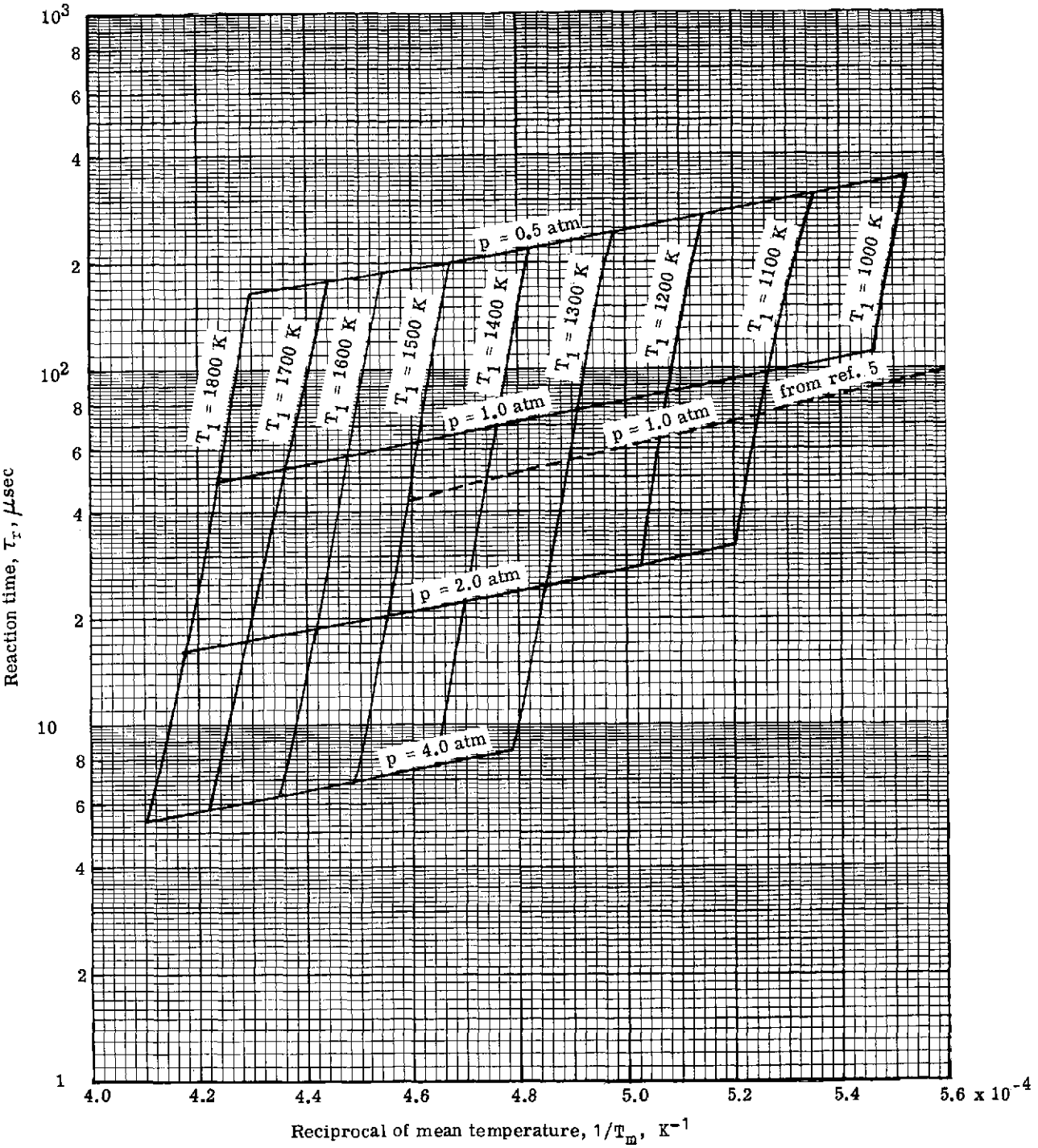

Figure 32.- Reaction time as a function of the reciprocal of mean temperature along isobars for $\phi = 1.0$ and $X_O = 0$ and 10^{-4}.

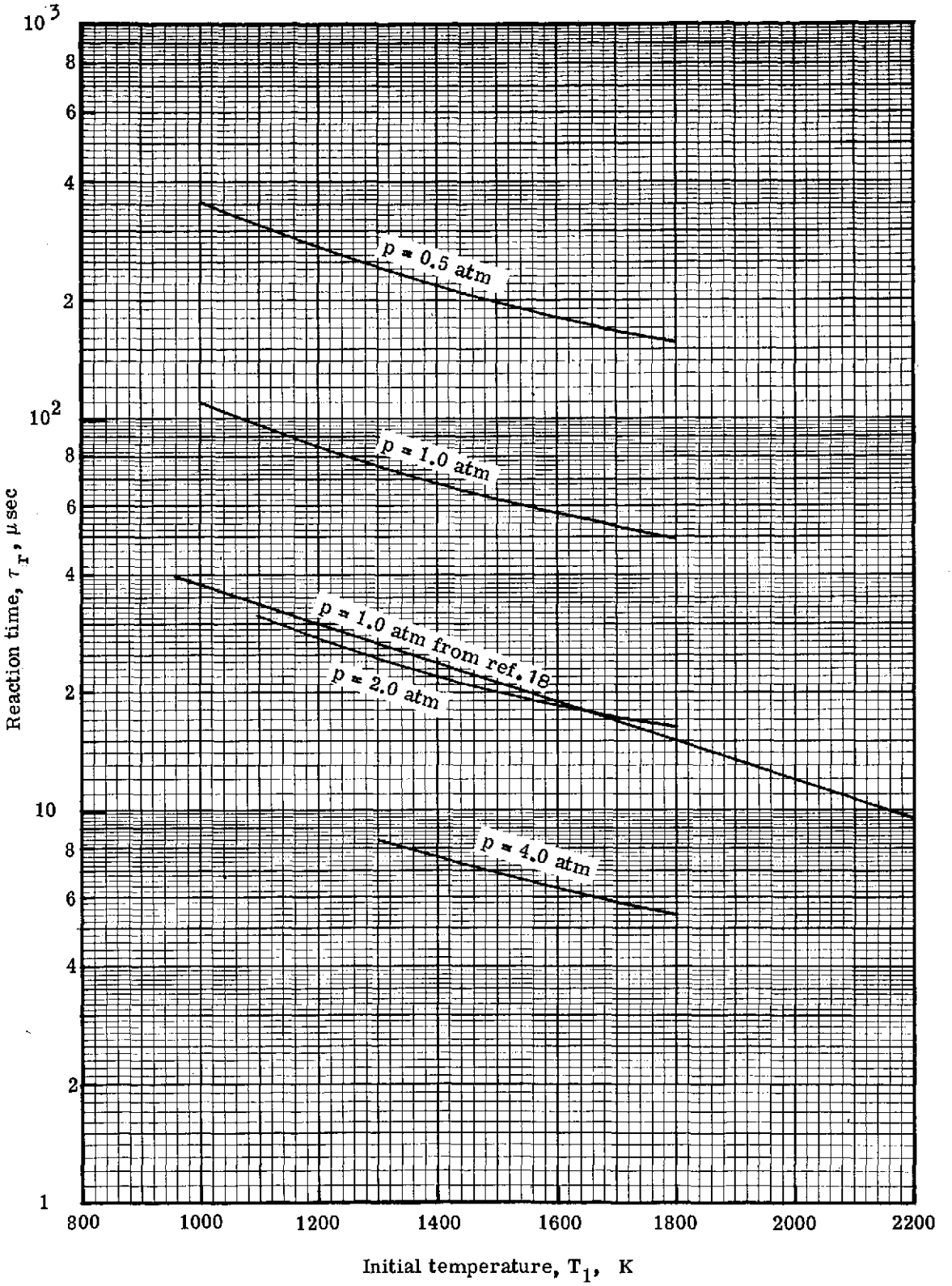

Figure 33.- Reaction time as a function of initial temperature along isobars for $\phi = 1.0$ and $X_O = 0$ and 10^{-4}.